Available online at www.sciencedirect.com
ScienceDirect
Virology 373 (2008) 447–456
VIROLOGY
www.elsevier.com/locate/yviro

Comparison of anti-viral activity of rhesus monkey and cynomolgus monkey TRIM5αs against human immunodeficiency virus type 2 infection

Ken Kono, Haihan Song, Yasuhiro Shingai, Tatsuo Shioda, Emi E. Nakayama *

Department of Viral Infections, Research Institute for Microbial Diseases, Osaka University, 3-1, Yamada-oka, Suita-shi, Osaka 565-0871, Japan

Received 9 November 2007; returned to author for revision 28 November 2007; accepted 17 December 2007
Available online 21 February 2008

Abstract

Human immunodeficiency virus type 2 (HIV-2) strains vary widely in their ability to grow in Old World monkey (OWM) cells. We previously evaluated several HIV-2 isolates for their sensitivity to cynomolgus monkey (CM) TRIM5α, an anti-HIV factor in OWM cells, and found that viruses carrying proline at the 120th position of the capsid protein were sensitive to CM TRIM5α, whereas those with either alanine or glutamine were resistant. In the study presented here, we tested these HIV-2 isolates for their sensitivity to rhesus monkey (Rh) TRIM5α and found that both CM TRIM5α-sensitive and -resistant viruses were restricted by Rh TRIM5α. The variable region 1 of the SPRY domain of Rh TRIM5α appeared to be the determinant of this difference. Furthermore, a mutagenesis study showed that three amino acid residues TFP at the 339th to 341st positions of Rh TRIM5α are important for restricting HIV-2 strains resistant to CM TRIM5α.

Keywords: TRIM5α; Human immunodeficiency virus; Rhesus monkey; Cynomolgus monkey

Introduction

Human immunodeficiency virus type 1 (HIV-1) has a very narrow host range limited to humans and chimpanzees. Experiments have demonstrated that HIV-1 does not infect Old World monkeys (OWM) such as rhesus and cynomolgus monkeys. Recently, the screening of a rhesus monkey cDNA library identified tripartite motif 5α (TRIM5α) as a factor that confers resistance to HIV-1 infection (Stremlau et al., 2004). Rhesus and cynomolgus monkey TRIM5α restricts HIV-1 infection (Stremlau et al., 2004; Yap et al., 2004; Nakayama et al., 2005), whereas human TRIM5α restricts N-tropic murine leukemia virus (N-MLV) infection (Hatziioannou et al., 2004; Keckesova et al., 2004; Perron et al., 2004). African green monkey (AGM) TRIM5α restricts simian immunodeficiency virus isolated from a macaque monkey (SIVmac), human immunodeficiency virus type 2 (HIV-2), and equine infectious anemia virus in addition to HIV-1 infection (Hatziioannou et al., 2004; Keckesova et al., 2004; Nakayama et al., 2005). TRIM5α shares with other splicing variants a common amino-terminal TRIM motif, comprising RING, B-box and coiled-coil domains, and encodes a unique SPRY (B30.2) domain (Reymond et al., 2001). Several recombinant studies of human and rhesus monkey TRIM5α have shown that the determinant of the species specificity lies in the SPRY domain of TRIM5α (Perez-Caballero et al., 2005; Sawyer et al., 2005; Stremlau et al., 2005; Yap et al., 2005). We also previously demonstrated that 17-amino-acid residues and adjacent AGM-specific 20-amino-acid duplication in the SPRY domain determined species-specific restriction of SIVmac (Nakayama et al., 2005). It is known that the RING and B-box domains are required for restriction and that the coiled-coil domain is required for multimerization (Stremlau et al., 2004; Berthoux et al., 2005; Perez-Caballero et al., 2005; Nakayama et al., 2006). TRIM5α is thought to bind HIV capsid and promote its rapid, premature disassembly in ubiquitin dependent

* Corresponding author. Fax: +81 6 6879 8347.
E-mail address: cmien@biken.osaka-u.ac.jp (E.E. Nakayama).

0042-6822/$ - see front matter © 2007 Elsevier Inc. All rights reserved.
doi:10.1016/j.virol.2007.12.022

and independent manners (Stremlau et al., 2006; Diaz-Griffero et al., 2006; Wu et al., 2006; Anderson et al., 2006). This means that the viral RNA and proteins are exposed to cellular proteins and degraded before nuclear transportation.

HIV-2 has a genome extremely similar to that of SIVmac (Hahn et al., 2000). In contrast with the many reports concerning HIV-1 and SIVmac, there have been only a few on susceptibility of HIV-2 to TRIM5α from various species (Nakayama et al., 2005; Ylinen et al., 2005). We previously evaluated eight HIV-2 isolates for their sensitivity to cynomolgus monkey TRIM5α and found that viruses carrying proline at the 119th or 120th position of the capsid protein (CA) were sensitive to cynomolgus monkey TRIM5α, whereas those with either alanine or glutamine were resistant (Song et al., 2007). In the study presented here, we tested these HIV-2 isolates for their sensitivity to another OWM rhesus monkey TRIM5α and found that both cynomolgus monkey TRIM5α-sensitive and -resistant viruses were restricted by rhesus monkey TRIM5α. We were able to show that three amino acid residues TFP at the 339th to 341st positions of rhesus monkey TRIM5α are important for restriction activity against HIV-2 strains.

Results

Rhesus monkey TRIM5α inhibits both cynomolgus monkey TRIM5α-sensitive and -resistant HIV-2 viruses

We previously reported that HIV-2 isolates carrying proline at the 120th position of CA were sensitive to cynomolgus monkey TRIM5α, whereas those with either alanine or glutamine were resistant. Both cynomolgus and rhesus monkey TRIM5αs are known to restrict HIV-1 but not SIVmac. Predicted amino acid sequences of cynomolgus and rhesus monkey TRIM5α are shown in Fig. 1. Rhesus and cynomolgus monkey TRIM5α share 96.8% of amino acid residues. To test these HIV-2 isolates for their sensitivity to rhesus monkey TRIM5α, we constructed a recombinant Sendai virus (SeV) expressing rhesus monkey TRIM5α fused with the HA tag in the C-terminal. Western blot analysis using an antibody against HA-tag showed that rhesus monkey TRIM5α was expressed at similar levels to those of cynomolgus monkey TRIM5α in recombinant SeV infected human T-cell line MT4 cells (data not shown). Fluorescent microscopic observation confirmed that these TRIM5αs were detected in all the cells infected with recombinant SeVs (data not

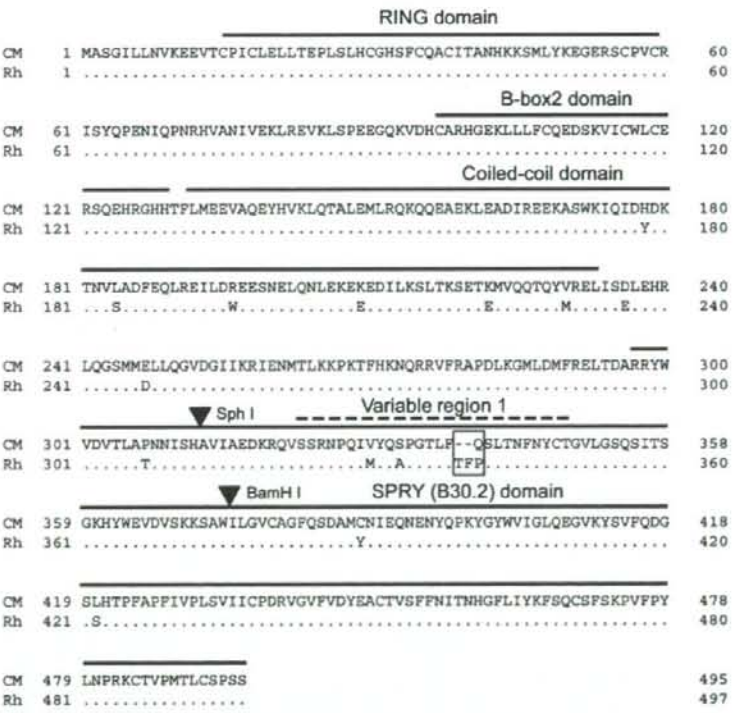

Fig. 1. Alignments of amino acid sequences of cynomolgus monkey (CM) and rhesus monkey (Rh) TRIM5αs. The RING, B-box2, coiled-coil and SPRY (B30.2) domains are indicated by labeled bars over the sequence. Variable region 1 is indicated by a broken bar over the sequence. Dots denote the amino acid residues identical to the one of cynomolgus monkey TRIM5α and dashes a lack of the amino acid residue that is present in rhesus monkey TRIM5α. The box marks amino acid residues that are important for rhesus monkey TRIM5α restriction activity against HIV-2 strains (see Results).

shown). We used SeV expressing cynomolgus monkey TRIM5α lacking the SPRY domain, CM SPRY(−) TRIM5α, as a negative control. MT4 cells infected with recombinant SeV expressing rhesus monkey TRIM5α, cynomolgus monkey TRIM5α, or CM SPRY(−) TRIM5α were then superinfected with an X4-tropic HIV-1 strain NL43, SIVmac239, HIV-2 strain GH123, or GH123/Q which is a mutant HIV-2 carrying glutamine (Q) at the 120th position of CA. In agreement with the results of previous studies, rhesus and cynomolgus monkey TRIM5α could restrict HIV-1 NL43, but failed to restrict SIVmac239 (Fig. 2, upper panels). HIV-2 GH123, cynomolgus monkey TRIM5α-sensitive strain, was restricted by both rhesus and cynomolgus monkey TRIM5αs (Fig. 2, lower left panel), which is also consistent with the findings of previous studies (Song et al., 2007). Despite a high degree of sequence similarity between rhesus and cynomolgus monkey TRIM5αs, rhesus monkey TRIM5α could inhibit replication of HIV-2 GH123/Q, the strain resistant to cynomolgus monkey TRIM5α (Fig. 2, lower right panel).

Variable region 1 (V1) of SPRY (B30.2) domain of rhesus monkey TRIM5α is a determinant for restriction of HIV-2 GH123/Q infection

It is known that the variable region 1 (V1) (Song et al., 2005a,b) of the rhesus monkey TRIM5α SPRY domain is the major determinant of anti-HIV-1 potency (Perez-Caballero et al., 2005; Sawyer et al., 2005; Stremlau et al., 2005; Yap et al., 2005). To determine the precise region of TRIM5α responsible for the anti HIV-2 GH123/Q activity of rhesus monkey TRIM5α, we constructed a recombinant SeV expressing chimeric TRIM5αs between rhesus and cynomolgus monkey TRIM5α by using *Sph*I and *Bam*HI restriction enzyme digestion (Fig. 3A). The central fragment comes from *Sph*I and *Bam*HI digestion contains the V1 of SPRY domain (Fig. 1).

As expected, all forms of chimeric TRIM5α inhibited HIV-1 NL43 and HIV-2 GH123 replication, although the extent of inhibition of HIV-2 GH123 varied among chimeric TRIM5αs (Fig. 3B, left and center panel). On the other hand, 212, 112, and 211 chimeric TRIM5α restricted HIV-2 GH123/Q infection, whereas 121, 221, and 122 chimeric TRIM5α did not (Fig. 3B, right panel), although the expression levels of the latter 1 day after SeV infection were not lower than those of parental and other chimeric TRIM5αs (Fig. 3C). Furthermore, these chimeric TRIM5α expression levels at day 6 after SeV infection were almost equivalent to those at day 1 after SeV infection (data not shown). These results confirmed that stability and kinetics of expression were similar among these chimeric TRIM5αs. Since 212,112, and 211 chimeric TRIM5α possess the rhesus monkey TRIM5α V1, those results indicated that the rhesus monkey TRIM5α V1 is a determinant of anti HIV-2 GH123/Q activity. It is noteworthy that cynomolgus monkey TRIM5α-sensitive HIV-2 GH123 grew to slightly higher titers in the cells

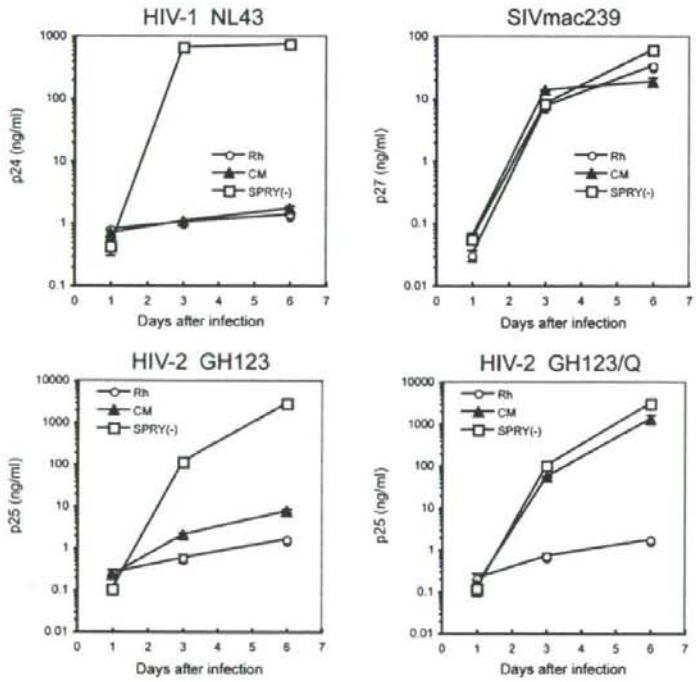

Fig. 2. MT4 cells infected with recombinant SeV expressing rhesus monkey (Rh; ○), cynomolgus monkey (CM; ▲), or CM SPRY(−) (□) TRIM5α were inoculated with HIV-1 NL43, SIVmac239, HIV-2 GH123, or HIV-2 GH123/Q. Culture supernatants were respectively assayed for levels of p24, p27, or p25. HIV-2 GH123/Q is a mutant virus carrying glutamine (Q) at the 120th position of HIV-1 GH123 capsid. CM SPRY(−) TRIM5α served as negative control.

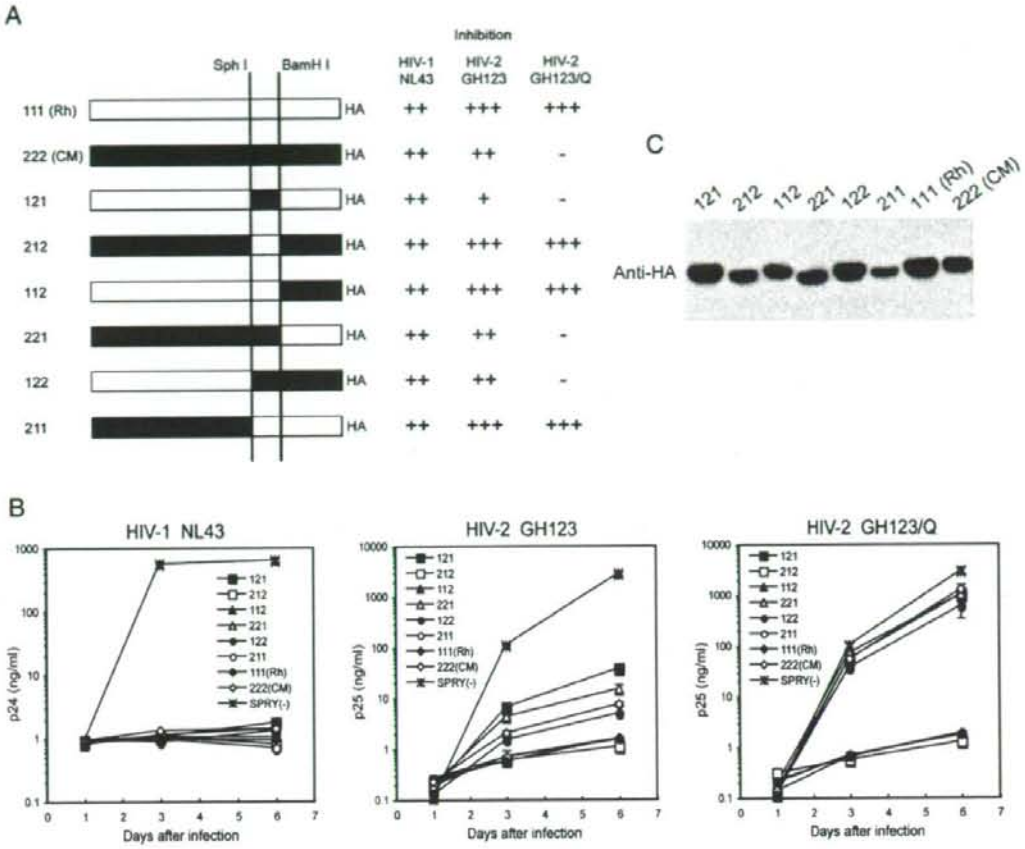

Fig. 3. (A) Schematic representation of chimeric TRIM5αs and summary of the results. White and black bars denote rhesus monkey (Rh) and cynomolgus monkey (CM) sequences, respectively. +++, ++, +, and − denote more than 1000-fold, 100- to 1000-fold, 8- to 100-fold, and less than 8-fold suppression of virus growth, respectively, compared with the negative control on day 6. (B) MT4 cells were infected with recombinant SeV expressing 121 (■), 212 (□), 112 (▲), 221 (△), 122 (●), 211 (○), 111 (Rh) (♦), 222 (CM) (◇), or CM SPRY(−) (*) TRIM5α. Nine hours after infection, cells were inoculated with HIV-1 NL43, HIV-2 GH123, or HIV-2 GH123/Q viruses. Culture supernatants were respectively assayed for levels of p24 or p25. (C) Twenty-four hours after SeV infection, TRIM5α proteins in lysates of MT4 cells infected with recombinant SeV expressing 121, 212, 112, 221, 122, 211, 111 (Rh), or 222 (CM) TRIM5α were visualized by Western blotting with an antibody against HA-tag.

expressing chimeric 121 or 221 TRIM5α than in those expressing parental cynomolgus monkey or 122 chimeric TRIM5α (Fig. 3B, center panel). These results indicate that the extent of inhibition of HIV-2 GH123 by chimeric 121 and 221 TRIM5αs is slightly less than that by parental cynomolgus monkey and 122 chimeric TRIM5α. It has been reported that all three variable regions (V1–V3) could contribute to the anti-viral activity of TRIM5α (Ohkura et al., 2006). It is possible that the combination of the cynomolgus monkey TRIM5α V1 and the rhesus monkey TRIM5α C-terminal portion of the SPRY domain slightly impairs the anti-HIV-2 function of TRIM5α.

V1 of SPRY domain of rhesus monkey TRIM5α is a determinant for broader and more potent anti-HIV-2 activity

To examine the restriction activities of rhesus monkey TRIM5α against other HIV-2 strains, we tested HIV-2 UC2, HIV-2 UC12, and HIV-2 UC14 for their growth potential in human T-cell line Hut78 infected with SeV expressing 121, 212, 111 (rhesus monkey; Rh), 222 (cynomolgus monkey; CM), or SPRY(−) TRIM5α. As shown in Fig. 4, rhesus monkey TRIM5α and cynomolgus monkey chimeric TRIM5α containing the V1 of rhesus monkey TRIM5α (212) completely restricted HIV-2 UC2 and HIV-2 UC14, whereas cynomolgus monkey TRIM5α and rhesus monkey chimeric TRIM5α containing the V1 of cynomolgus monkey TRIM5α (121) failed to do so. Rhesus monkey TRIM5α and 212 chimeric TRIM5α also completely restricted HIV-2 UC12, while cynomolgus monkey TRIM5α did so partially, which is consistent with our previous findings (Song et al., 2007). 121 chimeric TRIM5α showed very weak restriction activity on replication of HIV-2 UC12. Putting these findings together leads us to conclude that the V1 is a determinant for broader and more potent anti-HIV-2 activity of rhesus monkey TRIM5α.

Amino acid residues TFP at the 339th to 341st positions of rhesus monkey TRIM5α are important for inhibiting HIV-2 GH123/Q replication

As shown in Fig. 1, the V1 of the SPRY domain of rhesus monkey TRIM5α contains two amino acid residues TF that are not present in cynomolgus monkey TRIM5α. To examine whether these two additional amino acid residues are responsible for the broad anti-HIV-2 activity of rhesus monkey TRIM5α, we constructed a recombinant SeV expressing rhesus monkey TRIM5α lacking these two amino acid residues (Rh deltaTF TRIM5α). We also constructed a SeV expressing mutant rhesus monkey TRIM5α in which amino acid residues TFP at the 339th to 341st positions were replaced with a single amino acid Q found in cynomolgus monkey TRIM5α (Rh TFP-Q TRIM5α) (Fig. 5A). Expression levels of mutant TRIM5αs in MT4 cells infected with these SeVs were comparable to those of parental TRIM5αs (Fig. 5B).

As shown in Fig. 5C, both of the mutant rhesus monkey TRIM5αs restricted HIV-1 infection. In the case of HIV-2, Rh deltaTF TRIM5α inhibited both HIV-2 GH123 and HIV-2 GH123/Q replications, although anti-HIV-2 activity was slightly weaker than that of parental rhesus monkey TRIM5α. On the other hand, Rh TFP-Q TRIM5α lost its inhibitory activity against HIV-2 GH123/Q, while it could suppress replication of HIV-2 GH123 to the same extent as it was suppressed by 121 chimeric TRIM5α. Conversely, cynomolgus monkey TRIM5α possessing TFP instead of Q at the 339th position (CM Q-TFP TRIM5α) completely restricted HIV-2 GH123/Q replication (Fig. 5D). These results indicated that these three amino acids are important for restricting HIV-2 GH123/Q by rhesus monkey TRIM5α.

Baboon TRIM5α V1 confers anti-viral activity against HIV-2 GH123/Q to cynomolgus monkey TRIM5α, whereas sooty mangabey and pig-tailed monkey TRIM5α V1 fail to do so

HIV-2 is thought to originate from the simian immunodeficiency virus of sooty mangabeys (Hahn et al., 2000). Several HIV-2 isolates could grow in baboon and pig-tailed monkey, and some of them were reported to cause an AIDS-like disease in these animals (Barnett et al., 1994; Locher et al., 1998; Locher et al., 2001; McClure et al., 2000). To assess anti-HIV-2 activity of these OWMs TRIM5αs, we constructed a recombinant SeV expressing cynomolgus monkey chimeric TRIM5α containing the V1 of baboon (2B2), sooty mangabey (2S2), or pig-tailed monkey (2P2) TRIM5α (Fig. 6A). Expression levels of these chimeric TRIM5αs in MT4 cells infected with the SeVs were comparable to those of parental cynomolgus monkey TRIM5α (Fig. 6C). The amino acid sequences of the V1 of baboon, sooty mangabey, and pig-tailed monkey TRIM5α are shown in Fig. 6B. Baboon and sooty mangabey TRIM5α show the SFP sequence at the 339th to 341st positions, whereas pig-tailed monkey TRIM5α has a single Q as cynomolgus monkey TRIM5α. As shown in Fig. 6D, all the chimeric TRIM5αs containing the V1 of baboon, sooty mangabey, and pig-tailed monkey TRIM5α restricted HIV-1 infection. These results are consistent with those of previous studies (Kaiser et al., 2007; Newman et al., 2006; Ohkura et al., 2006). In the case of HIV-2, there were wide variations in anti-HIV-2 activity by the chimeric TRIM5αs. Chimeric TRIM5α containing baboon V1 inhibited both HIV-2 GH123 and HIV-2 GH123/Q replications, while chimeric TRIM5α containing sooty mangabey V1 partially inhibited HIV-2 GH123 and only slightly inhibited HIV-2 GH123/Q replication. Finally, chimeric TRIM5α containing pig-tailed monkey V1 only slightly inhibited both HIV-2 GH123 and HIV-2 GH123/Q replication. This shows that there is a lack of correlation between the effects of various TRIM5αs on HIV-2

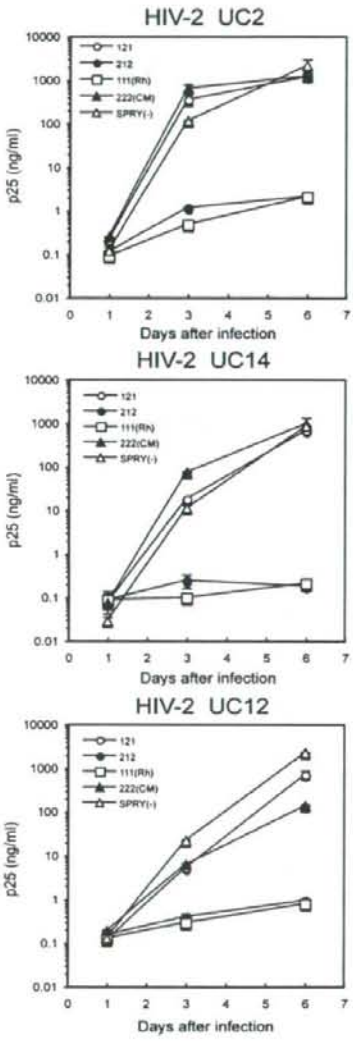

Fig. 4. Hut78 cells infected with recombinant SeV expressing 121 (○), 212 (●), 111 (Rh) (□), 222 (CM) (▲) or CM SPRY(−) (△) TRIM5α. Cells were super-infected with HIV-2 isolates, UC2, UC14, or UC12. Culture supernatants were assayed for levels of p25.

A

	Amino acid sequence	Inhibition HIV-1 NL43	HIV-2 GH123	HIV-2 GH123/Q
Rh	QIMTQAPGTLFTFPSLN	++	+++	+++
CM	..V..S.....--Q...	++	++	-
Rh deltaTF	.....--.....	++	++	++
Rh TFP-Q	.....--Q...	++	++	-
CM Q-TFP	..V..S.....	++	+++	+++

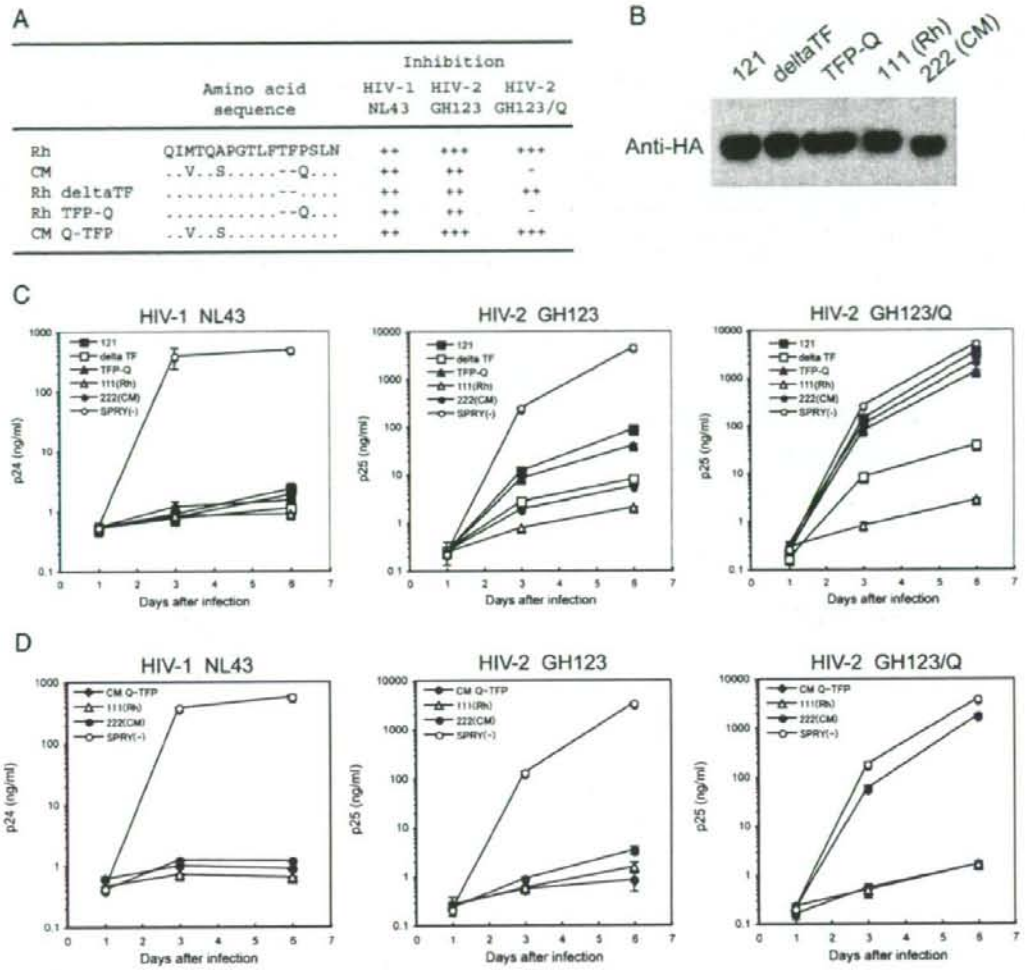

Fig. 5. (A) Mutant Rh deltaTF TRIM5α was generated by deleting 339th-TF-340th and mutant Rh TFP-Q TRIM5α was generated by replacing 339th-TFP-341st with Q by site-directed mutagenesis. Dots denote amino acid identity, dashes a lack of the amino acids residue present only in rhesus monkey (Rh) TRIM5α, and +++, ++, +, and − more than 1000-fold, 100- to 1000-fold, 8- to 100-fold, and less than 8-fold suppression of virus growth, respectively, compared with the negative control on day 6. (B) Twenty-four hours after SeV infection, TRIM5α proteins in lysates of MT4 cells infected with recombinant SeV expressing 121, Rh delta TF, Rh TFP-Q, 111 (Rh), or 222 (CM) TRIM5α were visualized by Western blotting with an antibody against HA-tag. (C) MT4 cells were infected with recombinant SeV expressing 121 (■), Rh delta TF (□), Rh TFP-Q (▲), 111 (Rh) (△), 222 (CM) (●), or CM SPRY(−) (○) TRIM5α. Nine hours after infection, cells were inoculated with HIV-1 NL43, HIV-2 GH123, or HIV-2 GH123/Q viruses. Culture supernatants were respectively assayed for levels of p24 or p25. (D) MT4 cells were infected with recombinant SeV expressing CM Q-TFP (♦), 111 (Rh) (△), 222 (CM) (●), or CM SPRY(−) (○) TRIM5α. Nine hours after infection, cells were inoculated with HIV-1 NL43, HIV-2 GH123, or HIV-2 GH123/Q viruses. Culture supernatants were respectively assayed for levels of p24 or p25.

and their reported ability to grow in these primate peripheral blood mononuclear cells.

Discussion

In the study presented here, we found that rhesus monkey TRIM5α showed anti-HIV-2 activity broader and more potent than that of cynomolgus monkey. We were also able to show that three amino acid residues TFP at the 339th to 341st positions in the V1 were important for the broad HIV-2 restriction activity of rhesus monkey TRIM5α. Previous studies have shown that the V1 of TRIM5α determines species-specific restriction of HIV-1 and SIVmac (Perez-Caballero et al., 2005; Sawyer et al., 2005; Stremlau et al., 2005; Yap et al., 2005; Nakayama et al., 2005). Ours is the first study to demonstrate that the V1 of TRIM5α also determines anti-HIV-2 potency. Since MT4 and Hut78 cells express endogenous human TRIM5α, it is possible that endogenous human TRIM5α interfere with exogenous TRIM5α. However, the expression level of SeV-derived TRIM5α is more than 100 times higher than that of endogenous TRIM5α (data

not shown), and the effect of endogenous TRIM5α is therefore considered to be negligible.

A previous study using a human and rhesus monkey chimeric TRIM5α revealed that a single amino acid substitution from R to P at the 332nd position of human TRIM5α (corresponding to the 334th position in rhesus monkey TRIM5α) confers strong anti-HIV-1 activity to human TRIM5α (Stremlau et al., 2005; Yap et al., 2005). We found that rhesus monkey TRIM5α and chimeric TRIM5α containing baboon V1 strongly restricted HIV-2 GH123/Q, while chimeric TRIM5α containing sooty mangabey V1 did so only slightly, although baboon and sooty mangabey TRIM5α share the SFP motif at the 339th to 341st positions. Rhesus monkey and baboon TRIM5α possess P, whereas human and sooty mangabey TRIM5α possess R at the 334th position. On the other hand, cynomolgus monkey TRIM5α strongly restricted HIV-2 GH123, while chimeric TRIM5α containing pig-tailed monkey V1 did so only slightly. Cynomolgus monkey TRIM5α possesses P, whereas pig-tailed monkey TRIM5α possesses Q at the 334th position. These results indicate the P residue at the 334th position of primate TRIM5α also plays a critical role in the restriction of HIV-2.

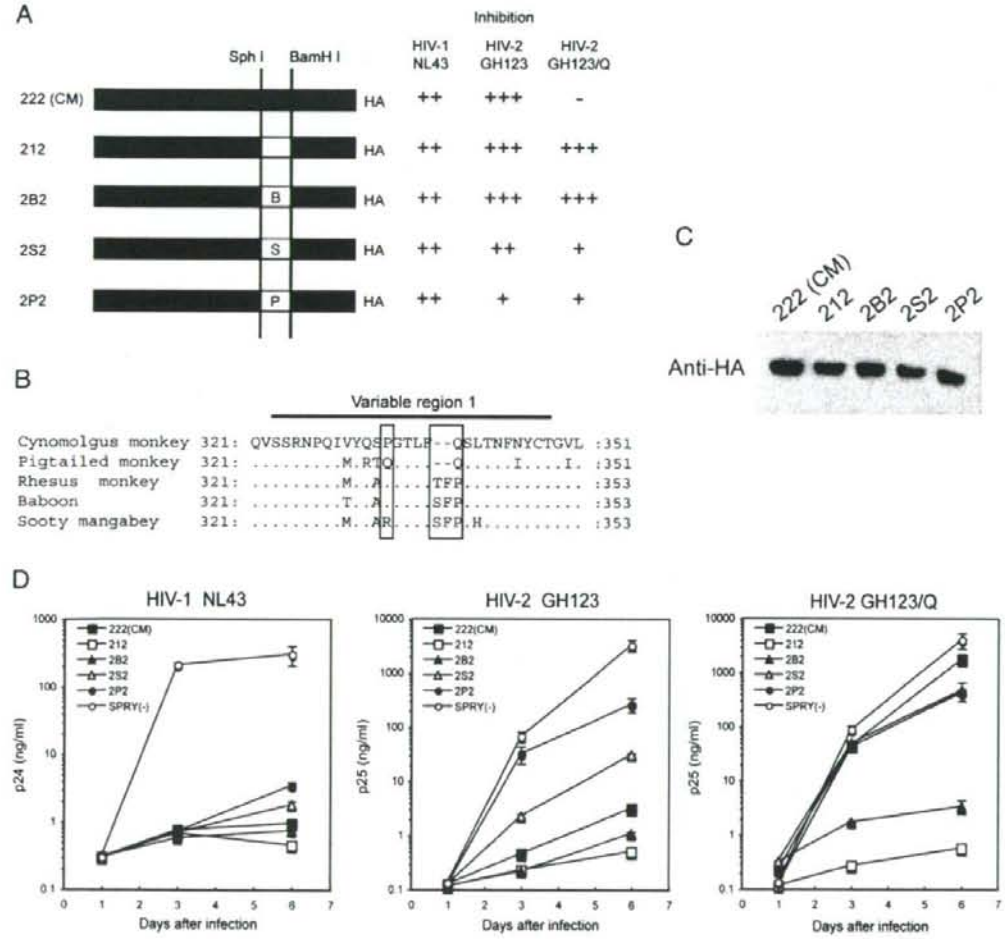

Fig. 6. (A) Schematic representation of chimeric TRIM5α and summary of the results. White and black bars denote rhesus monkey and cynomolgus monkey (CM) sequences, respectively. B, S, and P denote sequence from baboon, sooty mangabey, and pig-tailed monkey, respectively, and +++, ++, +, and − more than 1000-fold, 100- to 1000-fold, 8- to 100-fold, and less than 8-fold suppression of virus growth, respectively, compared with the negative control on day 6. (B) Alignment of amino acid sequences of the V1 and franking region within the SPRY domain of cynomolgus monkey, pigtailed monkey, rhesus monkey, baboon, and sooty mangabey TRIM5αs. V1 is indicated by a bar over the sequence. The first box indicates the amino acid residues that were referred to as site 332 in the human TRIM5α. The second box indicates amino acid residues that are important for restricting HIV-2 strains which are resistant to cynomolgus monkey TRIM5α. (C) Twenty-four hours after SeV infection, TRIM5α proteins in lysates of MT4 cells infected with recombinant SeV expressing 222 (CM), 212, 2B2, 2S2, or 2P2 TRIM5α were visualized by Western blotting with an antibody against HA-tag. (D) MT4 cells were infected with recombinant SeV expressing 222 (CM) (■), 212 (□), 2B2 (▲), 2S2 (△), 2P2 (●), or CM SPRY(−) (○) TRIM5α. Nine hours after infection, cells were inoculated with HIV-1 NL43, HIV-2 GH123, or HIV-2 GH123/Q, viruses. Culture supernatants were respectively assayed for levels of p24 or p25.

HIV-2 is thought to have originated from the SIV from sooty mangabey (SIVsmm) (Hahn et al., 2000). Our results showed that HIV-2 GH123 replication was partially inhibited by chimeric TRIM5α containing sooty mangabey V1, while HIV-2 GH123/Q grew strongly in the presence of the chimeric TRIM5α. This result is consistent with the fact that all SIVsmm sequences in the Los Alamos database possess Q or A at the 119th or 120th position of CA (Song et al., 2007). On the other hand, chimeric TRIM5α containing sooty mangabey V1 has a strong anti-HIV-1 activity, even though it has R at the 334th position as in human TRIM5α. Sooty mangabey TRIM5α, on the other hand, possesses the SFP motif at the 339th to 341st positions. Yap et al. (2005) showed that human TRIM5α carrying the rhesus monkey sequence LFTFPSLT which included the TFP motif instead of the human sequence RYQTFV at the 335th to 340th positions could restrict HIV-1. These results thus indicate that the TFP or SFP motif at the 339th to 341st positions can confer anti-HIV-1 activity as well as the P residue at the 334th position.

In the case of pig-tailed monkey, which could develop an AIDS-like disease by HIV-2 (McClure et al., 2000), anti-HIV-2 activity of chimeric TRIM5α containing pig-tailed monkey V1 was very weak. Furthermore, after we completed this study, it was reported that pig-tailed monkeys lack expression of TRIM5α. Instead, pig-tailed monkeys express TRIM5θ and TRIM5$_{71}$, novel TRIM5 isoforms lacking anti-HIV-1 activity (Brennan et al., 2007). These findings are probably account for the fact that pig-tailed monkey can be used as an AIDS model.

Previous studies showed that rhesus monkey as well as baboon can be infected with HIV-2 (Dormant et al., 1989; Franchini et al., 1989; Nicol et al., 1989; Franchini et al., 1990; Castro et al., 1991), while the latter can also develop an AIDS-like disease as a result of HIV-2 infection (Barnett et al., 1994; Locher et al., 1998; Locher et al., 2001). In our study, however, rhesus monkey TRIM5α and chimeric TRIM5α containing baboon V1 could strongly inhibit HIV-2 replication. The reason why HIV-2 can replicate in rhesus monkey and baboon, even though the TRIM5α of these monkey species possesses strong anti-HIV-2 activity, is unclear at present. The presence of TRIM5α mRNA in cells of rhesus monkey and baboon cells has been confirmed (Stremlau et al., 2004; Kaiser et al., 2007). It is also known that TRIM5α exhibits a high degree of sequence variation even within species. In rhesus monkey, there is a 339th-TFP-341st to Q polymorphism which diminishes the anti HIV-2 GH123/Q activity of rhesus monkey TRIM5α (Newman et al., 2006) (Fig. 5). It is thus possible that rhesus monkey carrying this polymorphism in the TRIM5α gene could be infected with HIV-2 and that a number of baboons have similar polymorphisms. It would be interesting to investigate the effect of genetic polymorphisms in baboon TRIM5α on its restriction activity against HIV-2.

Materials and methods

Cloning and expression of TRIM5α

Rhesus monkey TRIM5α cDNA was amplified by RT-PCR of mRNA extracted from rhesus monkey kidney LLC-MK2 cells using 5′-GCGGCCGCTACTATGGCTTCTGG-3′ as the forward primer and 5′-GAATTCTCAAGAGCTTGGTGA-3′ as the reverse primer. Amplified products were then cloned into the vector pCR-2.1TOPO (Invitrogen, Carlsbad, CA) and the nucleotide sequence authenticity was verified. For generating rhesus monkey TRIM5α cDNA carrying an HA tag (YPYDVPDYAA) at its C-terminus (Rh-TRIM5α-HA), cloned rhesus monkey TRIM5α cDNA in pCR-2.1TOPO was used as a template for PCR-amplification with a primer (5′-TCAAGCAGCATAATCAGGAACATCATAAGGATAAGAGCTTGGTGAGCACAGAG-3′) containing a nucleotide sequence corresponding to the HA-tag (underline) fused with the C-terminal portion of TRIM5α. The C-terminal portion of TRIM5α fused with the HA-tag (*Bam*HI to *Not*I) and the N-terminal portion of TRIM5α (*Not*I to *Bam*HI) was assembled on a pCEP4 vector (Invitrogen). Construction of cynomolgus monkey TRIM5α carrying an HA tag at the C-terminus (CM-TRIM5α-HA) was described previously (Nakayama et al., 2005).

To generate 121 chimeric TRIM5α, the 188-bp *Sph*I–*Bam*HI fragment of rhesus monkey TRIM5α was replaced with the corresponding 182-bp *Sph*I–*Bam*HI fragment of cynomolgus monkey TRIM5α in the background of Rh-TRIM5α-HA. Conversely, the 182-bp *Sph*I–*Bam*HI fragment of cynomolgus monkey TRIM5α was replaced with the 188-bp *Sph*I–*Bam*HI fragment of rhesus monkey TRIM5α in the background CM-TRIM5α-HA to generate 212 chimeric TRIM5α. To generate 112 chimeric TRIM5α, the C-terminal portion of CM-TRIM5α-HA (*Bam*HI to *Not*I) and the N-terminal portion of rhesus monkey TRIM5α were assembled on a pcDNA3.1 (−) vector (Invitrogen). Conversely, the C-terminal portion of Rh-TRIM5α-HA (*Bam*HI to *Not*I) and the N-terminal portion of cynomolgus monkey TRIM5α (*Not*I to *Bam*HI) were assembled on a pcDNA3.1 (−) vector to generate 221 chimeric TRIM5α. To generate 122 chimeric TRIM5α, the C-terminal portion of CM-TRIM5α-HA (*Sph*I to *Not*I) and the N-terminal portion of rhesus monkey TRIM5α (*Not*I to *Sph*I) were assembled on a pcDNA3.1 (−) vector. Conversely, the C-terminal portion of Rh-TRIM5α-HA (*Sph*I to *Not*I) and the N-terminal portion of cynomolgus monkey TRIM5α (*Not*I to *Sph*I) were assembled on a pcDNA vector to generate 211 chimeric TRIM5α.

Mutant rhesus monkey TRIM5α lacking two amino acid residues TF at the 339th to 340th positions (Rh deltaTF TRIM5α), mutant rhesus monkey TRIM5α in which amino acid residues TFP at the 339th to 341st positions was replaced with a single amino acid Q found in cynomolgus monkey TRIM5α (Rh TFP-Q TRIM5α), and mutant cynomolgus monkey TRIM5α in which a single amino acid Q at the 339th position was replaced with three amino acid residues TFP found in rhesus monkey TRIM5α (CM Q-TFP TRIM5α) were generated by site-directed mutagenesis by PCR-mediated overlap primer exension method (Ho et al., 1989). Briefly, two DNA fragments with overlapping ends were generated by using the outer primers and the complementary primers with overlapping complementary nucleotides containing desired mutations. The resultant two fragments were combined in the subsequent fusion reaction in which the overlapping ends anneal, allowing the 3′ overlap of each strand to serve as a primer for 3′ extension of the complementary strand. The outer primers for generating Rh deltaTF

TRIM5α were 5′-GCGGCCGCTACTATGGCTTCTGG-3′ and 5′-GAATTCTCAAGAGCTTGGTGA-3′, and the complementary primers were 5′-GGGACATTATTTCCGTCACTCACG-3′ and 5′-CGTGAGTGACGGAAATAATGTCCC-3′. The outer primers were common in all cases of PCR-based mutagenesis of TRIM5α. The complementary primers for Rh TFP-Q TRIM5α were 5′-GGGACATTATTTCAATCACTCACG-3′ and 5′-CGTGAGTGATTGAAATAATGTCCC-3′ (underline; TFP-Q site), and 5′-GGACATTATTTACGTTTCCGTCACTCACG-3′ and 5′-CGTGAGTGACGGAAACGTAAATAATGTCC-3′ (underline; Q-TFP site) for CM Q-TFP TRIM5α.

2B2, 2S2, and 2P2 chimeric TRIM5α, which possessed the 188-bp *Sph*I–*Bam*HI fragment of baboon TRIM5α, 188-bp fragment of sooty mangabey TRIM5α, and 182-bp fragment of pig-tailed monkey TRIM5α, respectively, in the background of CM-TRIM5α-HA were generated by the same method as described above. To obtain *Sph*I–*Bam*HI fragments of baboon and sooty mangabey TRIM5αs, cloned rhesus monkey TRIM5α was used as a template for PCR-amplification with outer primers described above and complementary primers containing a nucleotide sequence corresponding to the 330th to 339th amino acid residues of baboon TRIM5α (5′-CAGATAACGTATCAGGCACCAGGGACATTATTTTCGTTTCCG-3′ and 5′-CGGAAACGAAAATAATGTCCCTGGTGCCTGATACGTTATCTG-3′) and the 334th to 343rd amino acid residues of sooty mangabey TRIM5α (5′-CAGGCACGAGGGACATTATTTTCGTTTCCGTCACACACGAAT-3′ and 5′-ATTCGTGTGTGACGGAAACGAAAATAATGTCCCTCGTGCCTG-3′), respectively. To obtain the *Sph*I–*Bam*HI fragment of pig-tailed TRIM5α, cloned cynomolgus monkey TRIM5α was used as a template for PCR-amplification with outer primers described above and complementary primers containing a nucleotide sequence corresponding to the 330th to 350th amino acid residues of pig-tailed monkey TRIM5α (5′-CAGTCACTCACGAATTTCATTTATTGTACTGGCATCCTGGGC-3′ and 5′-CGTGAGTGACTGAAATAATGTCCCTTGTGTCCGATACATTATCTG-3′). The entire coding sequences of those TRIM5α were then transferred to the *Not*I site of pSeV18+b(+). Recombinant SeVs carrying various TRIM5α were recovered according to a previously described method (Nakayama et al., 2005). The viruses passaged twice in embryonated chicken eggs were used as stock for all experiments.

Viral infection

2×10^5 MT4 or Hut78 cells were infected with SeV expressing each TRIM5α at a multiplicity of infection of 10 plaque-forming units per cell and incubated at 37 °C for 9 h. Cells were then superinfected with 20 ng of p24 of HIV-1 NL43, 20 ng of p27 of SIVmac239, or 20 ng of p25 of HIV-2 GH123, GH123/Q, or other HIV-2 isolates. The culture supernatants were collected periodically, and the level of p24, p27, or p25 was measured with a RETROtek antigen ELISA kit (ZeptoMetrix, Buffalo, NY).

Western blot analysis

MT4 cells infected with recombinant SeVs expressing HA-tagged TRIM5α proteins were lysed in lysis buffer (50 mM Tris–HCl, pH 7.5, 150 mM NaCl, 1% Nonident P40, 0.5% sodium deoxycholate). TRIM5α proteins in the lysates were subjected to sodium dodecyl sulfate-polyacrylamide gel electrophoresis (SDS-PAGE). Proteins in the gel were then electronically transferred to a membrane (Immobilion; Millipore, Billerica, MA). Blots were blocked and probed with anti-HA high affinity rat monoclonal antibody (Roche, Indianapolis, IN) overnight at 4 °C. Blots were then incubated with peroxidase-conjugated anti-rat IgG (American Qualex, San Clemente, CA), and bound antibodies were visualized with a Chemilumi-One chemiluminescent kit (Nacalai Tesque, Kyoto, Japan).

TRIM5α cDNA sequences

TRIM5α cDNA sequences for rhesus monkey (AY523632), cynomolgus monkey (AB210052), baboon (AY843505), sooty mangabey (AY10303), and pig-tailed monkey (AY899887–AY899893) were obtained from the GeneBank database.

Acknowledgments

The authors would like to thank Setsuko Bandou and Noriko Teramoto for their assistance. HIV-2 UC2, UC12, and UC14 viruses were kind gifts from Jay A. Levy. This work was supported by grants from the Human Health Foundation, the Ministry of Education, Culture, Sports, Science, and Technology, and the Ministry of Health, Labor and Welfare, Japan.

References

Anderson, J.L., Campbell, E.M., Wu, X., Vandegraaff, N., Engelman, A., Hope, T.J., 2006. Proteasome inhibition reveals that a functional preintegration complex intermediate can be generated during restriction by diverse TRIM5 proteins. J. Virol. 80, 9754–9760.

Barnett, S.W., Murthy, K.K., Herndier, B.G., Levy, J.A., 1994. An AIDS-like condition induced in baboons by HIV-2. Science 266, 642–646.

Berthoux, L., Sebastian, S., Sayah, D.M., Luban, J., 2005. Disruption of human TRIM5α antiviral activity by nonhuman primate orthologues. J. Virol. 79, 7883–7888.

Brennan, G., Kozyrev, Y., Kodama, T., Hu, S.L., 2007. Novel TRIM5 isoforms expressed by *Macaca nemestrina*. J. Virol. 81, 12210–12217.

Castro, B.A., Nepomuceno, M., Lerche, N.W., Eichberg, J.W., Levy, J.A., 1991. Persistent infection of baboons and rhesus monkeys with different strains of HIV-2. Virology 184, 219–226.

Diaz-Griffero, F., Li, X., Javanbakht, H., Song, B., Welikala, S., Stremlau, M., Sodroski, J., 2006. Rapid turnover and polyubiquitylation of the retroviral restriction factor TRIM5. Virology 349, 300–315.

Dormant, D., Livartowski, J., Chamaret, S., Guetard, D., Hein, D., Levaguresse, R., van de Moortelle, P.F., Larke, B., Gourmelon, P., Vazeux, R., Metivier, H., Flageat, J., Court, L., Hauw, J.J., Montagnier, L., 1989. HIV-2 in rhesus monkeys: serological, virological and clinical results. Intervirology 30, 59–65.

Franchini, G., Fargnoli, K.A., Giombini, F., Jagodzinski, L., De Rossi, A., Bosch, M., Biberfeld, G., Fenyo, E.M., Albert, J., Gallo, R.C., Wong-Staal, F., 1989. Molecular and biological characterization of a replication competent human immunodeficiency type 2 (HIV-2) proviral clone. Proc. Natl. Acad. Sci. U. S. A. 86, 2433–2437.

Franchini, G., Markham, P., Gard, E., Fargnoli, K., Keubaruwa, S., Jagodzinski, L., Robert-Guroff, M., Lusso, P., Ford, G., Wong-Staal, F., Gallo, R.C., 1990. Persistent infection of rhesus macaques with a molecular clone of human immunodeficiency virus type 2: evidence of minimal genetic drift and low pathogenetic effects. J. Virol. 64, 4462–4467.

Hahn, B.H., Shaw, G.M., De Cock, K.M., Sharp, P.M., 2000. AIDS as a zoonosis: scientific and public health implications. Science 287, 607–614.

Hatziioannou, T., Perez-Caballero, D., Yang, A., Cowan, S., Bieniasz, P.D., 2004. Retrovirus resistance factors Ref1 and Lv1 are species-specific variants of TRIM5α. Proc. Natl. Acad. Sci. U. S. A. 101, 10774–10779.

Ho, S.N., Hunt, H.D., Horton, R.M., Pullen, J.K., Pease, L.R., 1989. Site-directed mutagenesis by overlap extension using the polymerase chain reaction. Gene 77, 51–59.

Kaiser, S.M., Malik, H.S., Emerman, M., 2007. Restriction of an extinct retrovirus by the human TRIM5α antiviral protein. Science 316, 1756–1758.

Keckesova, Z., Ylinen, L.M., Towers, G.J., 2004. The human and African green monkey TRIM5α genes encode Ref1 and Lv1 retroviral restriction factor activities. Proc. Natl. Acad. Sci. U. S. A. 101, 10780–10785.

Locher, C.P., Barnett, S.W., Herndier, B.G., Blackbourn, D.J., Reyes-Teran, G., Murthy, K.K., Brasky, K.M., Hubbard, G.B., Reinhart, T.A., Haase, A.T., Levy, J.A., 1998. Human immunodeficiency virus-2 infection in baboons is an animal model for human immunodeficiency virus pathogenesis in humans. Arch. Pathol. Lab. Med. 122, 523–533.

Locher, C.P., Witt, S.A., Herndier, B.G., Tenner-Racz, K., Racz, P., Levy, J.A., 2001. Baboons as an animal model for human immunodeficiency virus pathogenesis and vaccine development. Immunol. Rev. 183, 127–140.

McClure, J., Schmidt, A.M., Rey-Cuille, M.A., Bannink, J., Misher, L., Tsai, C.C., Anderson, D.M., Morton, W.R., Hu, S.L., 2000. Derivation and characterization of a highly pathogenic isolate of human immunodeficiency virus type 2 that causes rapid CD4+ cell depletion in *Macaca nemestrina*. J. Med. Primatol. 29, 114–126.

Nakayama, E.E., Miyoshi, H., Nagai, Y., Shioda, T., 2005. A specific region of 37 amino acid residues in the SPRY (B30.2) domain of African green monkey TRIM5α determines species-specific restriction of simian immunodeficiency virus SIVmac infection. J. Virol. 79, 8870–8877.

Nakayama, E.E., Macgawa, H., Shioda, T., 2006. A dominant-negative effect of cynomolgus monkey tripartite motif protein TRIM5α on anti-simian immunodeficiency virus SIVmac activity of an African green monkey orthologue. Virology 350, 158–163.

Newman, R.M., Hall, L., Connole, M., Chen, G.L., Sato, S., Yuste, E., Diehl, W., Hunter, E., Kaur, A., Miller, G.M., Johnson, W.E., 2006. Balancing selection and the evolution of functional polymorphism in Old World monkey TRIM5α. Proc. Natl. Acad. Sci. U. S. A. 103, 19134–19139.

Nicol, I., Flamminio-Zola, G., Doubouch, P., Bernard, J., Snart, R., Jouffre, R., Reveil, B., Fouchard, M., Desportes, I., Nara, P., Gallo, R.C., Zagury, D., 1989. Persistent HIV-2 infection of rhesus macaque, baboon, and mangabeys. Intervirology 30, 258–267.

Ohkura, S., Yap, M.W., Sheldon, T., Stoye, J.P., 2006. All three variable regions of the TRIM5α B30.2 domain can contribute to the specificity of retrovirus restriction. J. Virol. 80, 8554–8565.

Perez-Caballero, D., Hatziioannou, T., Yang, A., Cowan, S., Bieniasz, P.D., 2005. Human tripartite motif 5α domains responsible for retrovirus restriction activity and specificity. J. Virol. 79, 8969–8978.

Perron, M.J., Stremlau, M., Song, B., Ulm, W., Mulligan, R.C., Sodroski, J., 2004. TRIM5α mediates the postentry block to N-tropic murine leukemia viruses in human cells. Proc. Natl. Acad. Sci. U. S. A. 101, 11827–11832.

Reymond, A., Meroni, G., Fantozzi, A., Merla, G., Cairo, S., Luzi, L., Riganelli, D., Zanaria, E., Messali, S., Cainarca, S., Guffanti, A., Minucci, S., Pelicci, P.G., Ballabio, A., 2001. The tripartite motif family identifies cell compartments. EMBO J. 20, 2140–2151.

Sawyer, S.L., Wu, L.I., Emerman, M., Malik, H.S., 2005. Positive selection of primate TRIM5α identifies a critical species-specific retroviral restriction domain. Proc. Natl. Acad. Sci. U. S. A. 102, 2832–2837.

Song, B., Gold, B., O'Huigin, C., Javanbakht, H., Li, X., Stremlau, M., Winkler, C., Dean, M., Sodroski, J., 2005a. The B30.2(SPRY) domain of the retroviral restriction factor TRIM5α exhibits lineage-specific length and sequence variation in primates. J. Virol. 79, 6111–6121.

Song, B., Javanbakht, H., Perron, M., Park, D.H., Stremlau, M., Sodroski, J., 2005b. Retrovirus restriction by TRIM5α variants from Old World and New World primates. J. Virol. 79, 3930–3937.

Song, H., Nakayama, E.E., Yokoyama, M., Sato, H., Levy, J.A., Shioda, T., 2007. A single amino acid of the human immunodeficiency virus type 2 capsid affects its replication in the presence of cynomolgus monkey and human TRIM5αs. J. Virol. 81, 7280–7285.

Stremlau, M., Owens, C.M., Perron, M.J., Kiessling, M., Autissier, P., Sodroski, J., 2004. The cytoplasmic body component TRIM5α restricts HIV-1 infection in Old World monkeys. Nature 427, 848–853.

Stremlau, M., Perron, M., Welikala, S., Sodroski, J., 2005. Species-specific variation in the B30.2(SPRY) domain of TRIM5α determines the potency of human immunodeficiency virus restriction. J. Virol. 79, 3139–3145.

Stremlau, M., Perron, M., Lee, M., Li, Y., Song, B., Javanbakht, H., Diaz-Griffero, F., Anderson, D.J., Sundquist, W.I., Sodroski, J., 2006. Specific recognition and accelerated uncoating of retroviral capsids by the TRIM5α restriction factor. Proc. Natl. Acad. Sci. U. S. A. 103, 5514–5519.

Wu, X., Anderson, J.L., Campbell, E.M., Joseph, A.M., Hope, T.J., 2006. Proteasome inhibitors uncouple rhesus TRIM5α restriction of HIV-1 reverse transcription and infection. Proc. Natl. Acad. Sci. U. S. A. 103, 7465–7470.

Yap, M.W., Nisole, S., Lynch, C., Stoye, J.P., 2004. Trim5α protein restricts both HIV-1 and murine leukemia virus. Proc. Natl. Acad. Sci. U. S. A. 101, 10786–10791.

Yap, M.W., Nisole, S., Stoye, J.P., 2005. A single amino acid change in the SPRY domain of human Trim5α leads to HIV-1 restriction. Curr. Biol. 15, 73–78.

Ylinen, L.M., Keckesova, Z., Wilson, S.J., Ranasinghe, S., Towers, G.J., 2005. Differential restriction of human immunodeficiency virus type 2 and simian immunodeficiency virus SIVmac by TRIM5α alleles. J. Virol. 79, 11580–11587.

SOCS1 is an inducible host factor during HIV-1 infection and regulates the intracellular trafficking and stability of HIV-1 Gag

Akihide Ryo[a,b,c], Naomi Tsurutani[d], Kenji Ohba[b,e], Ryuichiro Kimura[e,f], Jun Komano[b], Mayuko Nishi[a], Hiromi Soeda[a], Shinichiro Hattori[b], Kilian Perrem[g], Mikio Yamamoto[h], Joe Chiba[f], Jun-ichi Mimaya[i], Kazuhisa Yoshimura[j], Shuzo Matsushita[j], Mitsuo Honda[b], Akihiko Yoshimura[k], Tatsuya Sawasaki[l], Ichiro Aoki[a], Yuko Morikawa[d], and Naoki Yamamoto[b,c]

[a]Department of Pathology, Yokohama City University School of Medicine, 3-9 Fuku-ura, Kanazawa-ku, Yokohama 236-0004, Japan; [b]AIDS Research Center, National Institute of Infectious Diseases, 1-23-1 Toyama, Shinjuku-ku, Tokyo 162-8640, Japan; [d]Kitasato Institute for Life Sciences, Kitasato University, Shirokane 5-9-1, Minato-ku, Tokyo 108-8641, Japan; [e]Department of Molecular Virology, Graduate School of Medicine, Tokyo Medical and Dental University, 1-5-45 Yushima, Bunkyo-ku, Tokyo 113-8519, Japan; [f]Molecular Oncology Laboratory, Department of Pathology, Royal College of Surgeons in Ireland, Smurfit Building, Beaumont Hospital, Dublin 9, Ireland; [h]Department of Biochemistry II, National Defense Medical College, 3-2 Namiki, Tokorozawa-shi, Saitama 359-8513, Japan; [g]Department of Biological Science and Technology, Science University of Tokyo, 2641 Yamazaki, Noda, Chiba 278-8510, Japan; [i]Division of Hematology and Oncology, Shizuoka Children's Hospital, 860 Urushiyama, Aoi-ku, Shizuoka 420-8660, Japan; [j]Division of Clinical Retrovirology and Infectious Diseases, Center for AIDS Research, Graduate School of Medical Sciences, Kumamoto University, Kumamoto 860-0811, Japan; [k]Division of Molecular and Cellular Immunology, Medical Institute of Bioregulation, Kyushu University, Fukuoka 812-8582, Japan; and [l]Cell Free Science and Research Center, Ehime University, Ehime 790-8577, Japan

Edited by Robert C. Gallo, University of Maryland, Baltimore, MD, and approved November 19, 2007 (received for review May 24, 2007)

Human immunodeficiency virus type 1 (HIV-1) utilizes the macromolecular machinery of the infected host cell to produce progeny virus. The discovery of cellular factors that participate in HIV-1 replication pathways has provided further insight into the molecular basis of virus–host cell interactions. Here, we report that the suppressor of cytokine signaling 1 (SOCS1) is an inducible host factor during HIV-1 infection and regulates the late stages of the HIV-1 replication pathway. SOCS1 can directly bind to the matrix and nucleocapsid regions of the HIV-1 p55 Gag polyprotein and enhance its stability and trafficking, resulting in the efficient production of HIV-1 particles via an IFN signaling-independent mechanism. The depletion of SOCS1 by siRNA reduces both the targeted trafficking and assembly of HIV-1 Gag, resulting in its accumulation as perinuclear solid aggregates that are eventually subjected to lysosomal degradation. These results together indicate that SOCS1 is a crucial host factor that regulates the intracellular dynamism of HIV-1 Gag and could therefore be a potential new therapeutic target for AIDS and its related disorders.

AIDS | pathogenesis | drug target | lysozyme

Human immunodeficiency virus type 1 (HIV-1) infection is a multistep and multifactorial process mediated by a complex series of virus–host cell interactions (1, 2). The molecular interactions between host cell factors and HIV-1 are vital to our understanding of not only the nature of the resulting viral replication, but also the subsequent cytopathogenesis that occurs in the infected cells (3). The characterization of the genes in the host cells that are up- or down-regulated upon HIV-1 infection could therefore provide a further elucidation of virus–host cell interactions and identify putative molecular targets for the HIV-1 replication pathway (4).

The HIV-1 p55 Gag protein consists of four domains that are cleaved by the viral protease concomitantly with virus release. This action generates the mature Gag protein comprising the matrix (MA/p17), capsid (CA/p24), nucleocapsid (NC/p7), and p6 domains, in addition to two small spacer peptides, SP1 and SP2 (5, 6). The N-terminal portion of MA, which is myristoylated, facilitates the targeting of Gag to the plasma membrane (PM), whereas CA and NC promote Gag multimerization. p6 plays a central role in the release of HIV-1 particles from PM by interacting with the vacuolar sorting protein Tsg101 and AIP1/ALIX (7–9). Several recent studies have implicated the presence of host factors in the control of the intracellular trafficking of Gag. AP-3δ is a recently characterized endosomal adaptor protein that binds directly to the MA region of Gag and enhances its targeting to the multivesicular body (MVB) during the early stages of particle assembly (10). The *trans*-Golgi network (TGN)-associated protein hPOSH plays another role in Gag transport by facilitating the egress of Gag cargo vesicles from the TGN, where it assembles with envelope protein (Env) before transport to PM (11). Although the involvement of these host proteins in the regulation of intracellular Gag trafficking has been proposed, the detailed molecular mechanisms underlying this process are still not yet well characterized.

In our current work, we demonstrate that the suppressor of cytokine signaling 1 (SOCS1) directly binds HIV-1 Gag and facilitates the intracellular trafficking and stability of this protein, resulting in the efficient production of HIV-1 particles. These results indicate that SOCS1 is a crucial host factor for efficient HIV-1 production and could be an intriguing molecular target for future treatment of AIDS and related diseases.

Results

SOCS1 Is Induced upon HIV-1 Infection and Facilitates HIV-1 Replication via Posttranscriptional Mechanisms. We and others have shown that HIV-1 infection can alter cellular gene expression patterns, resulting in the modification of viral replication and impaired homeostasis in the host cells (4, 12). Hence, to elucidate further the genes and cellular pathways that participate in HIV-1 replication processes, we performed serial analysis of gene expression (SAGE) using either a HIV-1 or mock-infected human T cell line, MOLT-4 (12). Further detailed analysis of relatively low-abundance SAGE tags identified *SOCS1* as a preferentially up-regulated gene after HIV-1 infection. This finding was validated by both semiquantitative RT-PCR and immunoblotting analysis with anti-SOCS1 anti-

Author contributions: A.R. and N.T. contributed equally to this work; A.R., A.Y., Y.M., and N.Y. designed research; A.R., N.T., K.O., R.K., M.N., H.S., S.H., T.S., I.A., and Y.M. performed research; J.K., S.H., M.Y., J.C., J.-i.M., K.Y., S.M., M.H., and A.Y. contributed new reagents/analytic tools; A.R., N.T., K.O., M.N., H.S., K.P., M.Y., K.Y., S.M., T.S., I.A., Y.M., and N.Y. analyzed data; and A.R., K.P., and N.Y. wrote the paper.

The authors declare no conflict of interest.

This article is a PNAS Direct Submission.

Freely available online through the PNAS open access option.

[c]To whom correspondence may be addressed. E-mail: aryo@nih.go.jp or nyama@nih.go.jp.

This article contains supporting information online at www.pnas.org/cgi/content/full/0704831105/DC1.

www.pnas.org/cgi/doi/10.1073/pnas.0704831105

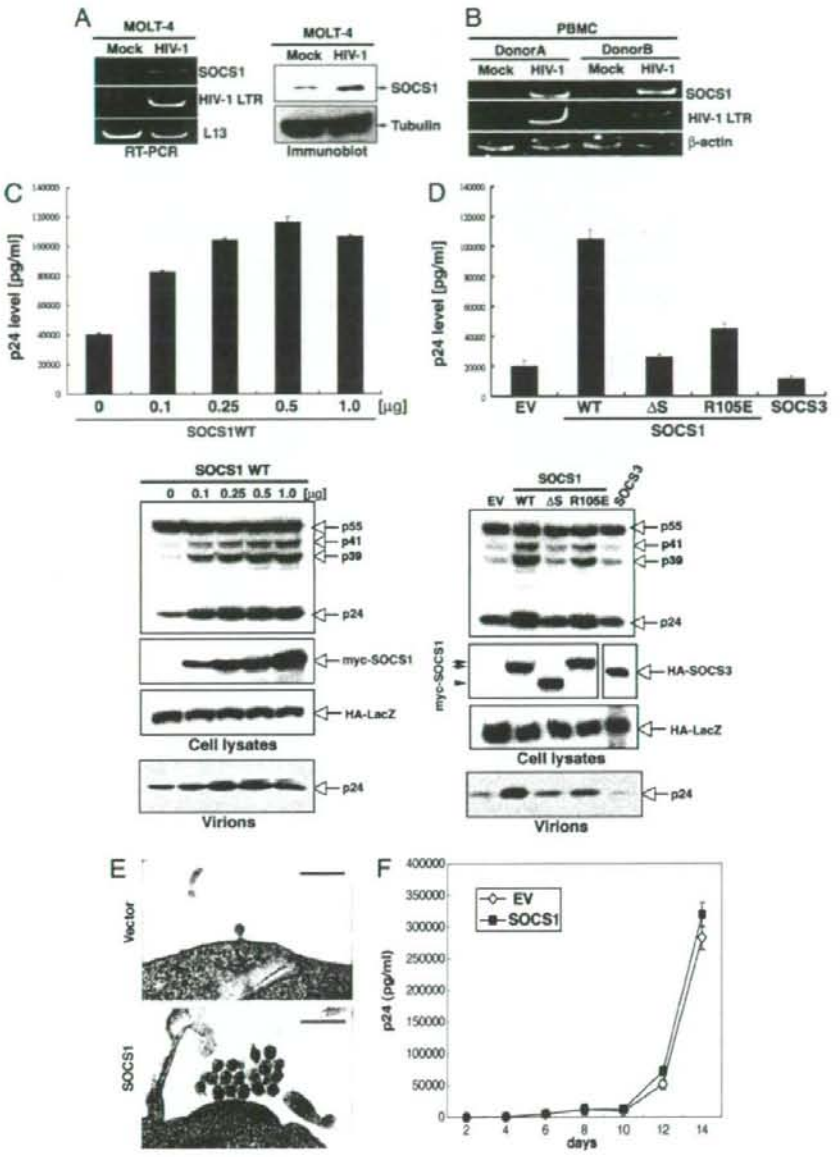

Fig. 1. SOCS1 is induced upon HIV-1 infection and enhances HIV-1 particle production. (*A*) MOLT-4 cells were mock-infected or infected with HIV-1_{NL4-3}, and then total RNA and protein extracts derived from these cells were subjected to semiquantitative RT-PCR (*Left*) and immunoblotting (*Right*), respectively. (*B*) PBMC from two healthy individuals were infected with HIV-1_{NL4-3} or were mock-infected, and SOCS1 expression was examined by semiquantitative RT-PCR. (*C*) 293T cells were transfected with pNL4-3 and cotransfected with various amounts of pcDNA-myc-SOCS1. Forty eight hours after transfection, p24 antigen release into the supernatant in each case was measured by antigen-capture ELISA (*Upper*), and the cell lysates and pelleted viruses were analyzed by immunoblotting (*Lower*). The data shown represent the mean ± SD from three independent experiments. HA-LacZ is a transfection control. (*D*) 293T cells were transfected with pNL4-3 and cotransfected with control vector, SOCS1 (WT), SOCS1ΔS (ΔSOCS box), SOCS1R105E, or SOCS3. Cell lysates and pelleted viruses were then collected after 48 h and subjected to ELISA (*Upper*) or immunoblotting (*Lower*), as described in *C*. (*E*) 293T cells cotransfected with either pNL4-3 plus control vector, or pNL4-3 plus myc-tagged SOCS1 were analyzed by TEM. Note that substantial numbers of mature virus particles can be observed in the myc-SOCS1-transfected cells. (Scale bars: 500 nm.) (*F*) Jurkat cells were infected with virions (adjusted by p24 levels) from either control vector (EV)- or SOCS1-transfected 293T cells. Supernatant p24 levels at the indicated time points were measured by ELISA.

bodies (Fig. 1*A*). In addition, *SOCS1* was found to be up-regulated also in peripheral blood mononuclear cells (PBMC) from two different individuals (following HIV infection, Fig. 1*B*).

Our initial findings that SOCS1 is induced upon HIV-1 infection prompted us to examine whether this gene product affects viral replication. We first cotransfected 293T cells with a HIV-1 infectious molecular clone, pNL4-3 (13), and also pcDNA-myc-SOCS1, and then monitored the virus production levels in the resulting supernatant. We then performed ELISA using an anti-p24 antibody and found that wild-type SOCS1 significantly increases the production of HIV-1 in the cell supernatant in a dose-dependent manner (Fig. 1*C Upper*). In contrast, neither the SH2 domain-defective mutant (R105E) nor the SOCS box deletion mutant (ΔS) of SOCS1 could promote virus production to the same levels as wild type, indicating that both domains are required for this enhancement (Fig. 1*D Upper*). Furthermore, another SOCS box protein, SOCS3, failed to augment HIV-1 replication in a parallel experiment (Fig. 1*D Upper*), indicating that the role of SOCS1 during HIV-1 replication is specific.

We next performed immunoblotting analysis using cell lysates and harvested virus particles in further parallel experiments (Fig. 1 *C* and *D Lower*). Consistent with our ELISA analysis, the expres-

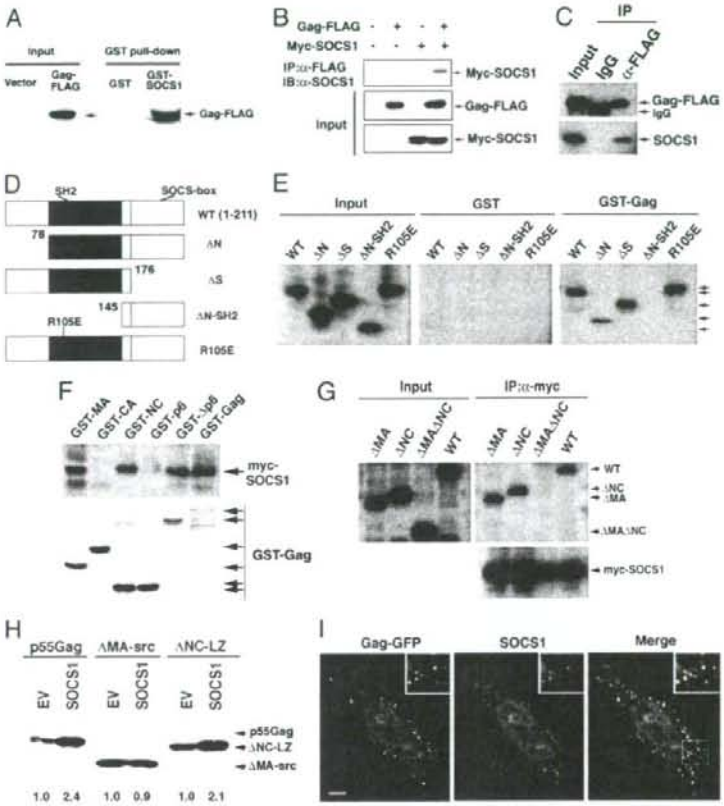

Fig. 2. SOCS1 interacts with HIV-1 Gag. (*A*) Extracts of 293T cells transfected with either empty vector or Gag-FLAG were subjected to pull-down analyses using glutathione–agarose beads with GST-SOCS1 in the presence of 10 ng/ml RNase followed by immunoblotting with anti-FLAG antibodies. (*B*) Extracts of 293T cells transiently expressing myc-SOCS1 and Gag-FLAG were subjected to immunoprecipitation (IP) with anti-FLAG monoclonal antibodies in the presence of 10 ng/ml RNase followed by immunoblotting (IB) analysis with either anti-FLAG or anti-myc polyclonal antibodies. (*C*) 293T cells were transiently transfected with Gag-FLAG, and cell lysates were then subjected to immunoprecipitation with anti-FLAG antibodies followed by immunoblotting with an antibody directed against endogenous SOCS1. (*D* and *E*) 293T cells expressing various myc-tagged SOCS1 mutants (schematically depicted in *D*) were analyzed by GST pull-down analysis with either GST or GST-Gag recombinant protein (*E*). (*F*) GST fusion proteins of the indicated regions of Gag were bound to glutathione beads and incubated with cell lysates from 293T cells expressing myc-SOCS1 in the presence of 10 ng/ml RNase followed by immunoblotting with anti-myc antibodies. (*G*) SOCS1 binds p55 Gag via either its MA or NC domains. 293T cells were transfected with myc-SOCS1 and cotransfected with Gag-FLAG, Gag.ΔMA-FLAG, Gag.ΔNC-FLAG, or Gag.ΔMA.ΔNC-FLAG. At 24 h after transfection, cell lysates treated with 10 μg/ml RNase were subjected to coimmunoprecipitation with anti-myc monoclonal antibodies followed by immunoblotting with anti-FLAG or anti-myc polyclonal antibodies. (*H*) Functional interaction of SOCS1 with MA but not NC. 293T cells were transfected with wild-type Gag, ΔMA-src, or ΔNC-LZ (Z_{IL}-p6) and cotransfected with either control vector or SOCS1. Supernatant virus particles were then collected after 24 h and subjected to immunoblotting with anti-p24 antibody. Numerical values below the blots indicate fold induction of supernatant p55 signal intensities derived by densitometry. (*I*) Colocalization of SOCS1 with Gag. HeLa cells were transiently transfected with Gag-GFP. After 24 h, the cells were fixed, permeabilized, and immunostained with anti-SOCS1 polyclonal antibody followed by fluorescently labeled secondary antibodies before confocal microscopy. (Scale bar: 10 μm.)

sion of wild-type SOCS1, but neither its SH2 nor SOCS box mutant counterparts, resulted in a marked and dose-dependent increase in the level of intracellular Gag protein, particularly in the case of CA (p24) and intermediate cleavage products corresponding to MA-CA (p41) and CA-NC (p39). This increase was found to be accompanied by an enhanced level of HIV-1 particle production in the supernatant (Fig. 1 *C* and *D Lower*). These results together indicated that SOCS1 facilitates HIV-1 particle production in infected cells and that this role of SOCS1 requires the function of both its SH2 and SOCS box domains. For further details about SOCS1 interaction with MA and NC and SOCS1-enhanced particle production, see supporting information (SI) *Text*.

To examine the morphological aspects of HIV-1 particle production, transmission electron microscopy (TEM) was performed. 293T cells that had been cotransfected with pNL4-3, and either a control vector or a SOCS1 expression construct, were subjected to TEM analysis after fixation in glutaraldehyde. In SOCS1-transfected cells, a significantly increased number of mature virus particles was observed on the surfaces of PM compared with the control vector-transfected cells (Fig. 1*E*). There were also no obvious malformations of the virus particles in SOCS1-expressing cells, such as doublet formation or tethering to PM, which are characteristic of particle budding arrest (14) (Fig. 1*E*). Consistent with this observation, virions from SOCS1-transfected cells were found to be infectious as control viruses in Jurkat cells when the same amounts of virus were infected (Fig. 1*F*). These results together indicate that SOCS1 enhances mature and infectious HIV-1 particle formation.

To elucidate the specific step in HIV-1 production that is enhanced by SOCS1, we next performed gene reporter assays using either luciferase expression constructs under the control of wild-type HIV-LTR (pLTR-luc), or a full-length provirus vector (pNL4-3-luc) (15). Interestingly, SOCS1 overexpression was found not to affect the transcription of these reporter constructs (data not shown), indicating that SOCS1 enhances HIV-1 replication via posttranscriptional mechanisms during virus production.

SOCS1 Interacts with the HIV-1 Gag Protein. The results of our initial experiments indicated that SOCS1 enhances HIV-1 production via a posttranscriptional mechanism. We therefore next tested whether SOCS1 could bind directly to HIV-1 Gag. GST pull-down analysis using C-terminal FLAG-tagged p55 Gag (codon-optimized) and GST-fused SOCS1 revealed that p55 Gag undergoes specific coprecipitation with GST-SOCS1 (Fig. 2*A*). Furthermore, both ectopically expressed myc-tagged SOCS1 and endogenous SOCS1 were found to undergo coimmunoprecipitation with Gag-FLAG in 293T cells (Fig. 2 *B* and *C*). Additionally, GST pull-down analysis with various SOCS1 mutants, as depicted in Fig. 2*D*, further demonstrated that a mutant lacking the both N-terminal and SH2 domain (ΔN-SH2) could not bind

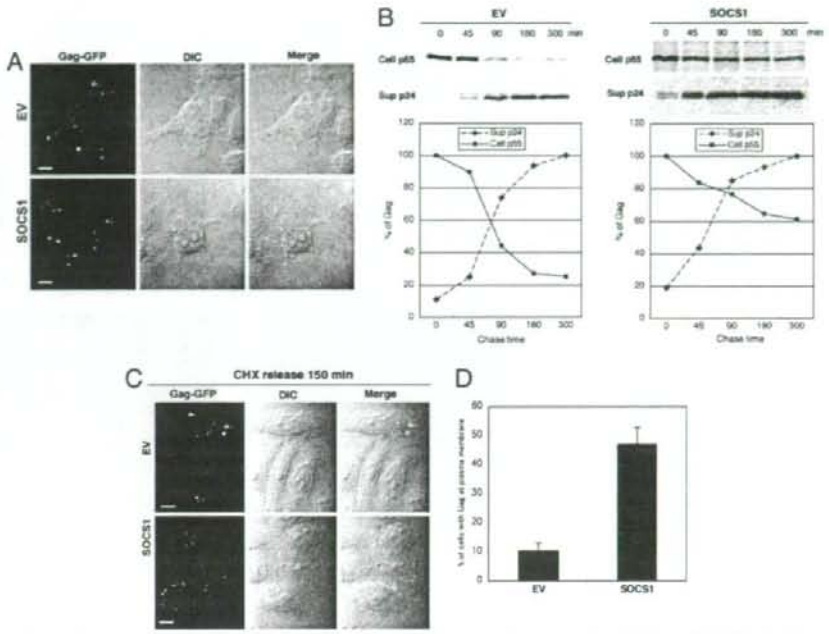

Fig. 3. SOCS1 enhances both the stability and trafficking of HIV-1 Gag. (*A*) HeLa cells cotransfected with pNL4-3 and either control vector (EV) or SOCS1 were immunostained with antibodies targeting anti-p24 (CA). Confocal microscopy with differential interference contrast (DIC) was then performed. (Scale bars: 10 μm.) (*B*) 293T cells were transfected with either a control empty vector (EV) (*Left*) or myc-SOCS1 (*Right*) and cotransfected with pNL4-3. After 48 h, cells were pulse-labeled with [^{35}S]methionine or [^{35}S]cysteine for 15 min and chased for the durations indicated. Cell lysates and pelleted supernatant virions were immunoprecipitated with anti-p24 antibodies followed by autoradiography. (*C* and *D*) HeLa cells seeded on poly-L-lysine-coated cover slides were transfected with either vector control or SOCS1. After 24 h, cells were again transfected with Gag-GFP for 3 h and then treated with 100 μg/ml CHX for 5 h to inhibit protein synthesis. This treatment was followed by incubation with fresh medium; then 150 min after the CHX release, cells were fixed and subjected to confocal microscopy (*C*). (Scale bars: 10 μm.) Cells with Gag protein on the plasma membrane were scored out of 200 transfected cells (*D*).

p55 Gag, whereas an N-terminal or a SOCS box deletion did not affect the binding of SOCS1 to Gag in 293T cells (Fig. 2*E*). This finding indicates that the SH2 domain is important for the interaction of SOCS1 with HIV-1 Gag. Interestingly, the R105E mutant of SOCS1, which disrupts the function of the SH2 domain, still binds Gag (Fig. 2*E*), indicating that the Gag–SOCS1 association is independent of the tyrosine phosphorylation of Gag, as is the case for both HPV-E7 and Vav (16, 17).

To elucidate the SOCS1-binding region of the Gag protein, GST pull-downs with various GST-fused Gag domain constructs were performed. SOCS1 was detected in glutathione bead precipitates with GST-wild-type Gag, GST-Δp6, GST-MA, and GST-NC, but not with other domain constructs (Fig. 2*F*), indicating that SOCS1 interacts with Gag via its MA and NC domains. Consistent with these results, the deletion of both the MA and NC domains of p55 Gag (ΔMAΔNC) completely abolishes its interaction with SOCS1 in coimmunoprecipitation experiments (Fig. 2*G*). Furthermore, *in vitro* analysis with purified proteins also demonstrated that SOCS1 can indeed interact with both the MA and NC regions of HIV-1 Gag in the absence of nucleic acids or other proteins (SI Fig. 5).

We next wished to determine the functional interaction domain in HIV-1 Gag through which SOCS1 functions in terms of virus-like particle production. To this end, we used a MA-deleted Gag mutant with an N-terminal myristoyl tag derived from src (ΔMA-src) (18) and also an NC-deleted Gag mutant with a GCN4 leucine zipper in place of NC, which we herein denote as ΔNC-LZ but which has been described as Z_{FL}-p6 (19). Both of these mutants have been shown still to assemble and bud (18, 19). We found that SOCS1 overexpression can still augment the particle formation of both wild-type Gag and ΔNC-LZ but not ΔMA-src (Fig. 2*H*), indicating that the functional interaction between SOCS1 and HIV-1 Gag is in fact mediated through MA.

To confirm further the direct interaction between SOCS1 and Gag in cells, we examined the intracellular localization of these two proteins. Confocal microscopy revealed that endogenous SOCS1 forms dotted filamentous structures in the cytoplasm and that Gag localizes in a very punctate pattern with SOCS1 from the perinuclear regions to the cell periphery (Fig. 2*I*). These data indicate that SOCS1 interacts with HIV-1 Gag in the cytoplasm during HIV-1 particle production.

SOCS1 Promotes both the Stability of Gag and Its Targeting to the Plasma Membrane. Because we had found from our initial data that SOCS1 increases HIV-1 particle production as a result of its direct interaction with intracellular Gag proteins, we next addressed whether SOCS1 positively regulates Gag stability and subsequent trafficking to PM. Our immunofluorescent analysis with the anti-p24 (CA) antibody initially revealed that SOCS1 overexpression increases the levels of Gag at PM when cotransfected with pNL4-3 at 48 h after transfection, although it was detected at PM in both control and SOCS1-expressing cells (Fig. 3*A*). Furthermore, the levels of cytoplasmic Gag were found to be much lower in the SOCS1-expressing cells compared with the control cells (Fig. 3*A*). These results indicate that SOCS1 enhances Gag trafficking to PM.

To examine next whether SOCS1 affects the stability and trafficking of newly synthesized Gag proteins, we performed pulse–chase analysis. This experiment revealed that SOCS1 significantly increases the stability of the intracellular p55 Gag polyprotein as well as the levels of p24 in the supernatant (Fig. 3*B*). Importantly, p24 was detectable at an earlier time point and reached maximum levels in a shorter period in the cell supernatant of SOCS1-transfected cells compared with control vector-transfected cells (Fig. 3*B*). This finding again suggests that SOCS1 facilitates the intracellular trafficking of newly synthesized Gag proteins to PM.

To confirm this hypothesis further, we performed cycloheximide (CHX) analysis with HeLa cells transfected using either vector control or SOCS1. After 24 h, cells were again transfected with Gag-GFP for 3 h and treated with CHX for 5 h to inhibit protein synthesis. Cells were then cultured in fresh medium without CHX for an additional 150 min and subjected to confocal microscopy. At

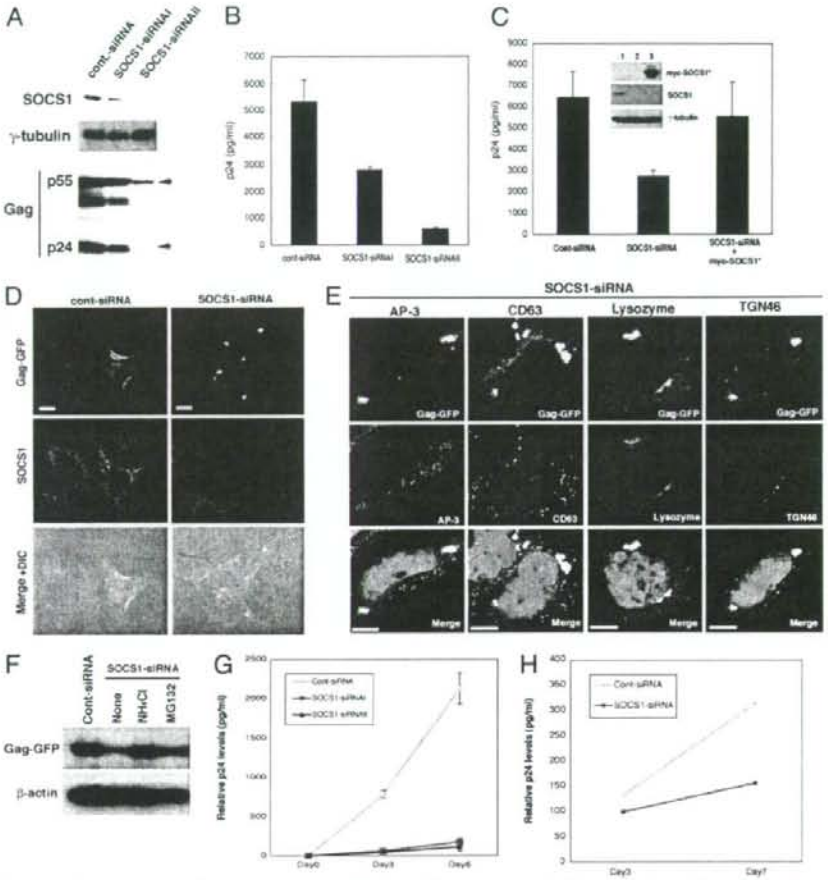

Fig. 4. The targeted inhibition of SOCS1 suppresses Gag trafficking and HIV-1 particle production and enhances Gag degradation in lysosomes. (*A* and *B*) 293T cells were transfected with either control siRNA or two different SOCS1-specific siRNAs (I or II) together with pNL4-3. At 48 h after transfection, cell lysates were subjected to immunoblotting analysis with the indicated antibodies (*A*). Cell supernatants were then subjected to ELISA analysis of p24 levels (*B*). (*C*) 293T cells were transfected with pNL4-3 and cotransfected with control-siRNA, SOCS1-siRNAI alone, or SOCS1-siRNAI plus siRNA-resistant myc-SOCS1 (myc-SOCS1*). After 48 h, cell supernatants were collected and subjected to p24 ELISA. (*Inset*) Immunoblots of the cell lysates. (*D*) HeLa cells were transfected with control or SOCS1-specific siRNA and cotransfected with GFP-Gag. At 48 h after transfection, the cells were subjected to confocal microscopy. (*E*) HeLa cells were transfected with Gag-GFP and SOCS1-siRNA constructs for 48 h. Cells were then fixed and subjected to immunofluorescent analysis with indicated antibodies followed by DAPI staining. (Scale bars: 10 mm.) (*F*) HeLa cells were transfected with Gag-GFP and cotransfected with either control-siRNA or SOCS1-siRNA. After 36 h, the cells were treated with a mock solution, 10 mM NH_4Cl or 10 μM MG132 for another 16 h. Cell were then harvested and subjected to immunoblotting analysis with anti-GFP or anti-β-actin antibodies. (*G*) Jurkat cells were infected with a retroviral vector encoding control (Cont) or two different SOCS1-specific siRNAs (I or II). After selection with puromycin, the cells were then infected with HIV-1_{NL4-3} (multiplicity of infection, 0.1), and p24 antigen levels in cell supernatant were measured by ELISA at the indicated time points. (*H*) Human primary CD4 T cells were separated from healthy donors and infected with lentivirus vectors encoding either control- or SOCS1-siRNAI. The cells were then infected with HIV-1_{NL4-3} (multiplicity of infection, 0.1), and p24 antigen levels in cell supernatant were measured by ELISA at the indicated time points.

this time point, Gag-GFP was found to localize predominantly in a perinuclear region in the control cells (Fig. 3*C*), whereas almost half of the SOCS1-transfected cells exhibited Gag-GFP localization on PM (Fig. 3*D*). These results again indicate that SOCS1 efficiently enhances the trafficking of newly synthesized Gag protein to PM.

The Targeted Disruption of SOCS1 Inhibits Gag Trafficking and HIV-1 Particle Production. To delineate further the role of SOCS1 in the trafficking of Gag and in subsequent HIV-1 particle production, we depleted cellular SOCS1 by siRNA. The significant depletion of SOCS1 expression by two different SOCS1-specific siRNA constructs was confirmed by immunoblotting analysis (Fig. 4 *A* and *B*). Significantly, in cells cotransfected with pNL4-3 and SOCS1-specific siRNAs, both HIV-1 particle release and the levels of intracellular Gag protein are significantly decreased compared with the control cells (Fig. 4 *A* and *B*). Furthermore, the effects of SOCS1-siRNA on the inhibition of HIV-1 particle production was diminished by reexpression with a codon-optimized SOCS1 construct that is resistant to these siRNAs (Fig. 4*C*), indicating that the SOCS1 siRNA suppression of HIV-1 particle production depends on the availability of endogenous SOCS1.

Consistent with these observations, immunofluorescent analysis further revealed that the expression of SOCS1-siRNA dramatically inhibits Gag trafficking such that Gag proteins accumulate in the perinuclear regions as large solid aggregates, as has been reported (20) (Fig. 4*D*). This finding indicates that SOCS1 plays an essential role in the Gag trafficking from perinuclear clusters to PM. Interestingly, these discrete perinuclear clusters of Gag were found to colocalize with lysosome markers, lysozyme, and partly with AP-3, but neither with the late endosome MVB marker CD63 nor the *trans*-Golgi marker TGN46, indicating that Gag is targeted for degradation by lysosomes when the function of SOCS1 is inhibited (Fig. 4*E*). In support of this notion, the levels of intracellular Gag were found to be significantly increased by treatment with a lysosome inhibitor NH_4Cl but not by a proteasome inhibitor MG132 in SOCS1-siRNA cells (Fig. 4*F*), further indicating that the perinuclear clusters of Gag will undergo lysosomal degradation rather than proteasomal degradation when optimal Gag transport to PM is suppressed by the inhibition of SOCS1.

We next addressed whether targeted SOCS1 inhibition would affect HIV-1 particle production in human T cells. The effect of SOCS1 depletion was clearly evident in both HIV-1_{NL4-3}-infected

Jurkat cells and human primary CD4+ T cells, which demonstrated pronounced decreases in virus particle production in SOCS1-siRNA-expressed cells compared with the controls (Fig. 4 *G* and *H*). These results together indicate that the specific inhibition of SOCS1 suppresses the optimal trafficking of Gag to PM, resulting in the degradation of Gag in lysosomes, which in turn leads to the efficient and reproducible inhibition of HIV-1 particle production in various types of human cells.

Discussion

In this work, we report that SOCS1 is an inducible host factor during HIV-1 infection and plays a key role in the late stages of the viral replication pathway via an IFN-independent mechanism (SI Fig. 6). These results represent evidence that SOCS1 is a potent host factor that facilitates HIV-1 particle production via posttranscriptional mechanisms.

SOCS1 has been shown to be a suppressor of several cytokine signaling pathways, and like all SOCS family members it has a central SH2 domain and a conserved C-terminal domain known as the SOCS box (21, 22). Structure–function analyses have further demonstrated that the SOCS1 SH2 domain is required for the efficient binding of its substrates (23, 24). Indeed, our current analyses have also revealed that the SH2 domain of SOCS1 is required for its interaction with the HIV-1 Gag protein. We have shown from our present data that the SOCS box is also required for SOCS1 to function during HIV-1 particle production.

The SOCS box-mediated function of SOCS1 is chiefly exerted via its ubiquitin ligase activity (21, 25). Biochemical binding studies have shown that the SOCS box of SOCS1 interacts with the elongin BC complex, a component of the ubiquitin/proteasome pathway that forms an E3 ligase with Cul2 (or Cul5) and Rbx-1 (21, 26, 27). We show from our current experiments that the SOCS box is required for HIV-1 particle production, indicating the involvement of the ubiquitin/proteasome pathway. However, it is still unknown whether SOCS1 promotes the ubiquitination of Gag and, if so, whether the mono- or poly-ubiquitination of Gag would affect its trafficking and protein stability. Further studies will be necessary to clarify the biological significance of Gag ubiquitination.

Perlman and Resh (20) recently reported that newly synthesized Gag first appears to be diffusely distributed in the cytoplasm, accumulates in perinuclear clusters, passes transiently through a MVB-like compartment, and then traffics to PM. Consistent with these observations, our current work also shows that Gag is accumulated at perinuclear clusters as solid aggregates when its targeting to PM is impaired because of the SOCS1 inhibition.

Another aspect of SOCS1 function during HIV-1 infection was proposed recently. Song *et al.* (28) reported that SOCS1-silenced dendritic cells broadly induce the enhancement of HIV-1 Env-specific CD8+ cytotoxic T lymphocytes and CD4+ T helper cells as well as an antibody response. The induction of the SOCS1 gene in HIV-1 infected cells might therefore disrupt a specific intracellular immune response to HIV-1 in infected host cells.

Based on the strong evidence that we present in our current work that SOCS1 positively regulates the late stages of HIV replication, we conclude that SOCS1 is likely to be a valuable therapeutic target not only for future treatments of AIDS and related diseases, but also for a postexposure prophylaxis against disease in HIV-1-infected individuals.

Materials and Methods

Antibodies and Fluorescent Reagents. Antibodies and fluorescent reagents were obtained from the following sources. Anti-CD63, anti-AP-3, anti-myc (A-14), and anti-SOCS1 (H-93) were from Santa Cruz Biotechnology. Anti-SOCS1 was from Zymed Laboratories. Anti-FLAG (M2) and anti-HA (12CA5) were from Sigma and Roche Diagnostics, respectively. Anti-HIV-p24 (Dako; Cytomation), anti-STAT1, and anti-phospho-STAT1 (Y701) were from BD Transduction Laboratories. Sheep polyclonal anti-TGN46 was from GeneTex.

Plasmid Constructs. Expression constructs for SOCS1 have been described in ref. 29. GST fusion constructs with specific regions derived from the codon-optimized *gag* were generated (MA, CA, NC, p6, Δp6, full-length Gag) by cloning into pGEX-2T (GE Healthcare Bio-Sciences) as described in ref. 30. For retrovirus-mediated siRNA expression, pSUPER.retro.puro vector was digested, as described in ref. 31, with the following sequences: SOCS1-siRNAI, TCGAGCTGCTGGAGCACTA; SOCS1-siRNAII, GGCCAGAACCTTCCTCCTCTT; control siRNA, TCGTATGTTGTGTGGAATT.

Electron Microscopy. Transfected 293T cells were fixed with 2.5% glutaraldehyde and subjected to TEM, as described (14, 32).

ACKNOWLEDGMENTS. We thank Dr. H Gottlinger (University of Massachusetts) for providing plasmids. This work was supported in part by grants from the Ministry of Education, Culture, Sports, Science, and Technology of Japan and Human Health Science of Japan.

1. Sorin M, Kalpana GV (2006) *Curr HIV Res* 4:117–130.
2. Freed EO (2004) *Trends Microbiol* 12:170–177.
3. Peterlin BM, Trono D (2003) *Nat Rev Immunol* 3:97–107.
4. Trkola A (2004) *Curr Opin Microbiol* 7:555–559.
5. Freed EO (1998) *Virology* 251:1–15.
6. Adamson CS, Jones IM (2004) *Rev Med Virol* 14:107–121.
7. VerPlank L, Bouamr F, LaGrassa TJ, Agresta B, Kikonyogo A, Leis J, Carter CA (2001) *Proc Natl Acad Sci USA* 98:7724–7729.
8. Garrus JE, von Schwedler UK, Pornillos OW, Morham SG, Zavitz KH, Wang HE, Wettstein DA, Stray KM, Cote M, Rich RL, *et al.* (2001) *Cell* 107:55–65.
9. Strack B, Calistri A, Craig S, Popova E, Gottlinger HG (2003) *Cell* 114:689–699.
10. Dong X, Li H, Derdowski A, Ding L, Burnett A, Chen X, Peters TR, Dermody TS, Woodruff E, Wang JJ, *et al.* (2005) *Cell* 120:663–674.
11. Alroy I, Tuvia S, Greener T, Gordon D, Barr HM, Taglicht D, Mandil-Levin R, Ben-Avraham D, Konforty D, Nir A, *et al.* (2005) *Proc Natl Acad Sci USA* 102:1478–1483.
12. Ryo A, Suzuki Y, Ichiyama K, Wakatsuki T, Kondoh N, Hada A, Yamamoto M, Yamamoto N (1999) *FEBS Lett* 462:182–186.
13. Adachi A, Gendelman HE, Koenig S, Folks T, Willey R, Rabson A, Martin MA (1986) *J Virol* 59:284–291.
14. Demirov DG, Ono A, Orenstein JM, Freed EO (2002) *Proc Natl Acad Sci USA* 99:955–960.
15. Chang TL, Mosoian A, Pine R, Klotman ME, Moore JP (2002) *J Virol* 76:569–581.
16. De Sepulveda P, Okkenhaug K, Rose JL, Hawley RG, Dubreuil P, Rottapel R (1999) *EMBO J* 18:904–915.
17. Kamio M, Yoshida T, Ogata H, Douchi T, Nagata Y, Inoue M, Hasegawa M, Yonemitsu Y, Yoshimura A (2004) *Oncogene* 23:3107–3115.
18. Gallina A, Mantoan G, Rindi G, Milanesi G (1994) *Biochem Biophys Res Commun* 204:1031–1038.
19. Accola MA, Strack B, Gottlinger HG (2000) *J Virol* 74:5395–5402.
20. Perlman M, Resh MD (2006) *Traffic* 7:731–745.
21. Alexander WS (2002) *Nat Rev Immunol* 2:410–416.
22. Marine JC, Topham DJ, McKay C, Wang D, Parganas E, Stravopodis D, Yoshimura A, Ihle JN (1999) *Cell* 98:609–616.
23. Narazaki M, Fujimoto M, Matsumoto T, Morita Y, Saito H, Kajita T, Yoshizaki K, Naka T, Kishimoto T (1998) *Proc Natl Acad Sci USA* 95:13130–13134.
24. Yasukawa H, Misawa H, Sakamoto H, Masuhara M, Sasaki A, Wakioka T, Ohtsuka S, Imaizumi T, Matsuda T, Ihle JN, *et al.* (1999) *EMBO J* 18:1309–1320.
25. Tyers M, Rottapel R (1999) *Proc Natl Acad Sci USA* 96:12230–12232.
26. Kamizono S, Hanada T, Yasukawa H, Minoguchi S, Kato R, Minoguchi M, Hattori K, Hatakeyama S, Yada M, Morita S, *et al.* (2001) *J Biol Chem* 276:12530–12538.
27. Kamura T, Burian D, Yan Q, Schmidt SL, Lane WS, Querido E, Branton PE, Shilatifard A, Conaway RC, Conaway JW (2001) *J Biol Chem* 276:29748–29753.
28. Song XT, Evel-Kabler K, Rollins L, Aldrich M, Gao F, Huang XF, Chen SY (2006) *PLoS Med* 3:e11.
29. Ryo A, Suizu F, Yoshida Y, Perrem K, Liou YC, Wulf G, Rottapel R, Yamaoka S, Lu KP (2003) *Mol Cell* 12:1413–1426.
30. Morikawa Y, Kishi T, Zhang WH, Nermut MV, Hockley DJ, Jones IM (1995) *J Virol* 69:4519–4523.
31. Ryo A, Uemura H, Ishiguro H, Saitoh T, Yamaguchi A, Perrem K, Kubota Y, Lu KP, Aoki I (2005) *Clin Cancer Res* 11:7523–7531.
32. Nagashima Y, Nishihira H, Miyagi Y, Tanaka Y, Sasaki Y, Nishi T, Imaizumi K, Aoki I, Misugi K (1996) *Cancer* 77:799–804.

JOURNAL OF VIROLOGY, Mar. 2008, p. 2528–2542 Vol. 82, No. 5
0022-538X/08/$08.00+0 doi:10.1128/JVI.02094-07

Human Immunodeficiency Virus Type 1 Vpr Inhibits Axonal Outgrowth through Induction of Mitochondrial Dysfunction▽

Hiroko Kitayama,[1] Yoshiharu Miura,[1] Yoshinori Ando,[1] Shigeki Hoshino,[2,3] Yukihito Ishizaka,[2] and Yoshio Koyanagi[1]*

Laboratory of Viral Pathogenesis, Institute for Virus Research, Kyoto University, Kyoto 606-8507, Japan[1]; Department of Intractable Diseases, International Medical Center of Japan, Tokyo 162-8655, Japan[2]; and Graduate School of Comprehensive Human Sciences, University of Tsukuba, Tsukuba 305-8577, Japan[3]

Received 21 September 2007/Accepted 12 December 2007

Human immunodeficiency virus type 1 (HIV-1)-infected macrophages damage mature neurons in the brain, although their effect on neuronal development has not been clarified. In this study, we show that HIV-1-infected macrophages produce factors that impair the development of neuronal precursor cells and that soluble viral protein R (Vpr) is one of the factors that has the ability to suppress axonal growth. Cell biological analysis revealed that extracellularly administered recombinant Vpr (rVpr) clearly accumulated in mitochondria where a Vpr-binding protein adenine nucleotide translocator localizes and also decreased the mitochondrial membrane potential, which led to ATP synthesis. The depletion of ATP synthesis reduced the transportation of mitochondria within neurites. This mitochondrial dysfunction inhibited axonal growth even when the frequency of apoptosis was not significant. We also found that point mutations of arginine (R) residues to alanine (A) residues at positions 73, 77, and 80 rendered rVpr incapable of causing mitochondrial membrane depolarization and axonal growth inhibition. Moreover, the Vpr-induced inhibition was suppressed after treatment with a ubiquinone analogue (ubiquinone-10). Our results suggest that soluble Vpr is a major viral factor that causes a disturbance in neuronal development through the induction of mitochondrial dysfunction. Since ubiquinone-10 protects the neuronal plasticity in vitro, it may be a therapeutic agent that can offer defense against HIV-1-associated neurological disease.

AIDS patients who have high levels of viral loads in the cerebrospinal fluid (CSF) tend to develop human immunodeficiency virus (HIV)-associated dementia (14, 31). Recently, attention has been brought to milder neurological diseases displayed in the antiretrovirus therapy-treated patients and healthy HIV-infected individuals (50). Mild neurocognitive disorder is defined as the presence of several cognitive deficits (14). In histopathological examinations of autopsy samples of HIV-1-infected brains, apoptosis in neurons was frequently found (2, 19). However, the frequency of apoptosis was low in patients displaying the milder neurological diseases (1). Although the molecules involved in HIV-associated neurological disturbance have not been completely identified, many data indicate that HIV type 1 (HIV-1)-infected macrophages or microglial cells produce neurotoxic factors such as viral products, excitotoxins, and/or cytokines (14, 20).

Viral proteins that are released from HIV-1-infected macrophages or microglial cells can be deleterious to the central nervous system (CNS). HIV-1 envelope glycoprotein 120 (gp120), transcriptional transactivator (Tat), and viral protein R (Vpr) have been shown to be toxic to neurons (14, 20). Recently, it has been reported that the HIV-1-induced inflammation caused by infiltrated macrophages might impede neuronal cell development in the hippocampus, as shown by a murine model of HIV-1 encephalopathy (43). However, it has not been shown that a viral protein released from HIV-1-infected macrophages can cause the retardation of neuronal development.

An HIV-1 accessory protein, Vpr, which is synthesized late in the HIV-1 replication cycle, is present in a soluble form in CSF and sera of HIV-1-infected patients displaying neurological disorders (34). It has been shown that Vpr causes many cellular dysfunctions, including cell cycle arrest at the G_2 phase caused by the induction of the damage-specific DNA-binding protein 1 (DDB1) and the Cullin 4A (Cul4A) E3 ubiquitin ligase pathway (8, 12, 13, 24, 33, 51, 56, 59) and the induction of caspase-dependent apoptosis (39). It is thought that HIV-1 Vpr is a potentially toxic molecule to mature neurons. In vitro studies using cultured neurons derived from rat hippocampal, cortical, and striatal neurons (42, 49) and an in vivo study using Vpr transgenic mice have shown that HIV-1 Vpr might have the potential to cause neuronal apoptosis (27). Furthermore, it is also known that Vpr-induced apoptosis is mediated by its binding to the adenine nucleotide translocator (ANT) in the inner membrane of mitochondria (25, 26, 48).

It has been shown that mitochondria play important roles in the establishment of axonal polarity and the regulation of neurite outgrowth during neuronal development (36). The trafficking of mitochondria may be a necessary task in neuronal development (10). However, the influence of HIV-1 Vpr on immature neurons, including neuronal progenitor cells, or its effect on neuronal plasticity has not been clarified.

Many pieces of evidence indicate that active neurogenesis occurs in parts of the adult brain, including the dentate gyrus (DG) of the hippocampus, the olfactory bulb, and the ventric-

* Corresponding author. Mailing address: Laboratory of Viral Pathogenesis, Institute for Virus Research, Kyoto University, 53 Shogoinkawara-cho, Sakyo-ku, Kyoto 606-8507, Japan. Phone: 81-75-751-4811. Fax: 81-75-751-4812. E-mail: ykoyanag@virus.kyoto-u.ac.jp.

▽ Published ahead of print on 19 December 2007.

ular epithelium, and is crucial for the formation of neuronal plasticity (35). Neural stem cells derived from DG differentiate into neurons and form synaptic networks, and these morphological and physiological features strongly suggest that the new neurons are incorporated into the hippocampal local circuitry and that they are involved in hippocampus-dependent memory formation and brain repair (35, 53, 57). The goal of this study was to identify the factors that damage neuronal development and to reveal the mechanisms of the inhibition of neuronal development that might cause the pathological alterations of HIV encephalopathy, including cognitive impairment in both pediatric patients and adult patients.

In this study, we examine whether HIV-1-infected macrophages inhibit neuronal cell development by using precursor cells isolated from murine fetal brain tissue. We discovered that soluble Vpr is one of the inhibitory factors of axonal growth and that it delays differentiation in precursor cells. Moreover, a subsequent detailed analysis of recombinant Vpr (rVpr)-treated cells revealed Vpr-induced mitochondrial membrane depolarization, which resulted in the disruption of ATP synthesis and the inhibition of mitochondrial transport in neurites of neuronal precursor cells. These negative effects were significantly suppressed in differentiation cultures and organotypic hippocampal slice cultures by ubiquinone-10 (UQ), which is a ubiquinone analogue that protects mitochondria from membrane depolarization. These data suggest that UQ is a therapeutic agent that can offer defense against the HIV-1-induced impairment of neuronal development.

MATERIALS AND METHODS

Preparation of CM from MDM. Neurobasal conditioned medium (CM) supplemented with Dulbecco's modified Eagle's medium (DMEM)-high glucose, 10% fetal calf serum, and B27 supplement (Invitrogen, Carlsbad, CA) was used to culture monocyte-derived macrophages (MDM) isolated from peripheral blood mononuclear cells of HIV-1-seronegative healthy donors. The MDM were left uninfected or were infected with HIV-1_{IRFP} (32) at a multiplicity of infection of 1.0. Five days after HIV-1 infection, culture supernatant was collected and the concentration of $p24^{CA}$ antigen (RETROtek; ZeptoMetrix, Buffalo, NY) and soluble Vpr protein (23) in each CM was measured by enzyme-linked immunosorbent assay (ELISA). Control CM, CM collected from uninfected MDM, and CM collected from infected MDM were designated C-CM, M-CM, and HIV-CM, respectively.

Preparation of rVpr and synthesized peptides. Wild-type rVpr (rVpr-WT) was purified as described previously (54). Three rVpr mutants that had alanine (A) instead of arginine (R) at position 80 (R80A), isoleucine (I) at position 81 (I81A), or arginine at positions 73, 77, and 80 (R73, 77, 80A) were prepared with the same procedure as that used for rVpr-WT. Four Vpr peptides were synthesized (Osaka Peptide Institute, Japan, and Wako Pure Chemicals, Japan).

Differentiation culture of neurons. The generation and maintenance of neurospheres from murine embryonic forebrains were performed as described previously (16). Briefly, cells were dissociated from the forebrains of embryonic day 15 ICR mice (Japan SLC, Inc., Japan). The experiments were carried out in accordance with the guidelines for animal experimentation at Kyoto University. Three days after the initiation of culture, neurospheres were separated into individual cells by trypsin-EDTA treatment and were plated onto glass coverslips (12 mm) precoated with poly-L-ornithine hydrochloride (Sigma-Aldrich, St. Louis, MO) and laminin from Engelbreth-Holm-Swarm murine sarcoma (Sigma-Aldrich) and were cultured with neurobasal CM. Phase-contrast images were acquired using a Leica CTR 6500 (Leica Microsystems, Heidelberg, Germany) with 20× and 40× objectives.

Measurement of neurite length and classification of developmental stages. Quantifications were performed using Leica FW4000 software (Leica Microsystems). To measure the length of neurites or axons, each neurite or axon from randomly chosen cells was traced manually from the proximal end to the distal end. To determine the percentage of cells in each developmental stage, randomly chosen cells were classified into three developmental stages based on their morphologies. Any progenitor cells that had an extended neurite (at least twice as long as other neurites by observation) were categorized as stage 3, and progenitor cells that do not have an extended neurite were categorized as stage 2. Progenitor cells that formed lamellipodia, which form small protrusion veils and a few spikes, were categorized as stage 1. The samples were prepared and blinded by one investigator. The measurement and classification were done by another investigator, to whom no information regarding the treatments was given. Experiments were repeated at least three times, and more than 100 adherent progenitor cells were analyzed for each independent experiment.

Vpr neutralization. To neutralize soluble Vpr in HIV-CM, progenitor cells were cultured in HIV-CM supplemented with mouse monoclonal anti-Vpr antibody (8D1; 260 ng/ml) (23) or mouse monoclonal anti-$p17^{MA}$ antibody (260 ng/ml; Advanced Biotechnologies, Columbia, MD).

Reagents. The following reagents were used: caspase-3 inhibitor (z-DEVD-fmk; BD Biosciences, San Diego, CA), UQ (Sigma-Aldrich), ATP (Sigma-Aldrich), and carbonyl cyanide 4-(trifluoromethoxy) phenylhydrazone (FCCP; Sigma-Aldrich).

Staining of mitochondria in live cells. To visualize mitochondria and calculate the velocity of mitochondrial transport in neurites or axons, cells were incubated with 100 nM MitoTracker Green FM (Invitrogen) by following the manufacturer's protocol. The temperature was maintained at 37°C with an air stream incubator. Cells were visualized with an oil immersion 63× objective on a confocal laser microscope (TCS SP2 AOBS; Leica Microsystems) using a 488-nm excitation wavelength for the quantification of mean pixels. The quantification of mean pixels was done by following the protocol supplied by the manufacturer (LCS Lite software; Leica Microsystems). To measure the velocity, images were acquired using a fluorescence microscope (Leica CTR 6500) using a green fluorescent protein (GFP) filter every 10 s for 120 s. The velocity of mitochondrial transport within neurites or axons was calculated by displacement (in micrometers) over time (in seconds). The mitochondrial membrane potential ($\Delta\Psi m$) was calculated using the fluorescent intensity of a $\Delta\Psi m$-sensitive dye, 5,5',6,6'-tetrachloro-1,1',3,3'-tetraethylbenzimidazolyl-carbocyanine iodide (JC-1; Invitrogen), by following the manufacturer's protocol. At 48 h of culture, cells were incubated with 1 μg/ml JC-1 at 37°C for 30 min and were visualized with an oil immersion 63× objective on a fluorescence microscope (Leica CTR 6500) using GFP and Texas Red filters. The temperature was maintained at 37°C with an air stream incubator. The red fluorescence intensity and green fluorescence intensity were measured using Leica FW4000 software. The normalized intensity ratio between green and red depends on $\Delta\Psi m$. $\Delta\Psi m$ (normalized JC-1 ratio) was calculated with the following formula: $\Delta\Psi m$ = (red fluorescence intensity − base fluorescence intensity)/(green fluorescence intensity − base fluorescence intensity).

ATP production assay. Cellular ATP levels were measured using the ATP bioluminescence assay kit HS II (Roche Applied Sciences, Indianapolis, IN). Briefly, cells were lysed in cell lysis reagent. Cell lysate and luciferase reagent then were added to microplates, and the luminescence was measured using a WALLAC ARVO SX 1420 multilabel counter (Perkin Elmer). The standard curve for ATP was obtained by measuring the luciferase intensity from a serially diluted standard ATP solution.

Isolation of mitochondria and Western blotting. The isolation of mitochondria in neuronal cells left untreated or treated with rVpr for 48 h was performed with the Oproteome mitochondria isolation kit (Qiagen, Hilden, Germany) by following the manufacturer's protocol. The cytosolic fraction was concentrated by acetone precipitation. Proteins from the mitochondrial fraction or cytosolic fraction or the whole-cell lysate were separated by sodium dodecyl sulfate–15% polyacrylamide gel electrophoresis, transferred onto a polyvinyl difluoride membrane (Immobilon transfer membranes; Millipore, Bedford, MA), and incubated with antibodies against cytochrome *c* (BD Biosciences), Vpr (23), and ANT (Santa Cruz Biotechnology, Santa Cruz, CA). Anti-mouse/rabbit immunoglobulin G (IgG) horseradish peroxidase-linked antibody (Cell Signaling Technology, Denver, MA) was used to detect the primary antibodies bound to the protein by using Western lighting chemiluminescence reagent (Perkin Elmer LAS, Boston, MA).

Slice cultures and retrovirus vector transduction. Organotypic hippocampal slices were prepared from postnatal 7-day-old Wistar Hannover GALAS rats (CLEA Japan, Inc.) as previously described (28). The slices were cultured on a porous translucent membrane (Millicell-CM; Millipore) at 34°C for 14 days. Slices were cocultured with HIV-1_{IRFL}-infected cells (multiplicity of infection, 1.0), uninfected MDM, or recombinant Vpr protein (23) across the porous membrane for 2 weeks. In some slices, an enhanced GFP (EGFP)-expressing murine leukemia virus (MLV)-based vector, SRα-EGFP (3), was inoculated in the suprapyramidal region of the dentate granule cell layer (GCL).

Immunocytochemistry and immunohistochemistry. The neuronal cells were fixed with paraformaldehyde (PFA) for 1 h at 4°C. After being washed, fixed cells were treated with phosphate-buffered saline (PBS) containing 5% normal goat serum (NGS) and 0.05% Triton X-100 at room temperature (RT) for 1 h, followed by incubation with mouse monoclonal anti-cytochrome c at RT for 2 h. Samples then were incubated with Alexa Fluor 488-conjugated anti-mouse IgG (Invitrogen) at RT for 2 h. Nuclei were stained using Hoechst 33342 (Invitrogen). The slices were fixed by immersion in 4% PFA for 1 h at 4°C. After being washed, slices were treated with buffer containing 5% NGS and 0.3% Triton X-100 (blocking solution) at 4°C overnight and then incubated with the following primary mouse monoclonal antibodies: anti-β-3-tubulin (B3T; Monosan, Uden, The Netherlands), neurofilament protein (NFP; DakoCytomation, Carpinteria, CA), microtubule-associated protein 2 (MAP2; Upstate, Lake Placid, NY), and neuronal nuclei (NeuN; Chemicon, Temecula, CA) at 4°C overnight in blocking solution. Samples subsequently were incubated at RT for 6 h with a fluorescent dye-conjugated secondary antibody (Alexa Fluor 594- or 488-conjugated anti-mouse IgG [Invitrogen]). Each sample was examined under a confocal laser microscope (TCS SP2 AOBS) with 40× and 63× objectives. The quantification of fluorescence intensity was done by following the protocol supplied by the manufacturer.

Statistical analysis. Data were generated from at least three replicate experiments. The statistical analysis was carried out by one-way analysis of variance. Multiple comparisons were performed with the Student's *t* test. A P value of less than 0.05 was considered significant.

RESULTS

Inhibition of axonal growth by HIV-1-infected MDM. To examine the effect of HIV-1-infected macrophages on neuronal development in vitro, we utilized differentiation cultures using neuronal progenitors derived from murine neurosphere cells. Neurite outgrowth in neurosphere cells apparently was hampered in the presence of CM of HIV-1_{JRFL}-infected MDM (HIV-CM) compared to the growth of those cultured in CM of uninfected MDM (M-CM) or in control CM (C-CM) (Fig. 1A). A similar inhibition was observed when we used progenitor cells isolated from murine fetal brain (data not shown). At 8 h of culture, the mean lengths of primary neurites were comparable among progenitor cells cultured in HIV-CM, M-CM, and C-CM (26.15 ± 8.94, 33.95 ± 4.84, and 34.90 ± 13.11 μm, respectively) (Fig. 1B), indicating that the initial steps of neurite generation are not affected. At 24 h of culture, however, the mean length of primary neurites in progenitor cells cultured in HIV-CM was less than those in progenitor cells cultured in M-CM or C-CM. As shown in Fig. 1B, at 72 h, the average length of the primary neurites of neuronal cells cultured with HIV-CM (52.20 ± 14.64 μm) was approximately one-third the length of those from cells cultured with M-CM or C-CM (169.70 ± 37.52 and 175.15 ± 34.14 μm, respectively).

We then evaluated polarity formation in progenitor cells cultured in HIV-CM, M-CM, and C-CM. When neuronal progenitor cells are plated, they initially form lamellipodia, which form small protrusion veils and a few spikes (stage 1). Following this event, several neurites of similar lengths extend (stage 2), leading to the formation of minor neurites. Finally, one of the neurites starts to grow rapidly, forming the primary neurite, while other neurites remain quiescent. This step is characterized by primary neurite outgrowth and axon formation, which results in the morphological polarization of the neuron (stage 3) (22). One hundred cells were randomly chosen from each CM and were classified into the three developmental stages according to their morphologies. When the progenitor cells were examined at 24 h, we found that more than half of them were in stage 2, independent of the CM (Fig. 1C). As shown in Fig. 1D, at 48 h the majority of progenitors cultured in C-CM and M-CM were in stage 3 (63.33% ± 0.58% and 55.33% ± 8.49%, respectively), but the majority of them were still in stage 2 in HIV-CM (64.00% ± 6.36%). These results indicate that the cells exposed to C-CM and M-CM had similar abilities to differentiate up to 72 h in culture and that the differentiation of HIV-CM-cultured progenitors was arrested at stage 2.

When HIV-CM with a low p24 concentration (below 200 pg/ml) was used, the inhibition of axon formation was not observed at 48 h (data not shown). However, when HIV-CM with a high HIV-1 p24 concentration (70.28 ± 21.6 ng/ml) was used, the inhibition was obvious, indicating the possibility that viral proteins are involved in the inhibition of axon formation. In fact, a relatively large amount of Vpr was detected in HIV-1 virion-free supernatant of HIV-CM (18.37 ± 7.54 pg/ml), as measured using ELISA. When the progenitor cells were cultured in HIV-CM in the presence of anti-Vpr antibody (8D1) (23), neurite outgrowth was clearly rescued at 72 h (Fig. 1E) and the number of neuronal cells scored at stage 3 clearly increased (Fig. 1F). On the other hand, no protective effect was observed in the anti-$p17^{MA}$ antibody-treated groups (Fig. 1E and F). These results suggest that Vpr produced from HIV-1-infected MDM played a role in the inhibition of axonal growth. As the recovery of neuronal cell differentiation was not complete, HIV-CM likely contains another inhibitory factor(s) against neurite outgrowth.

Inhibition of axonal outgrowth by soluble Vpr. To assess the direct effect of Vpr on axon formation, rVpr (23) was added to differentiation cultures of mouse neurosphere-dissociated progenitor cells. Since the highest concentration of soluble Vpr protein in HIV-1 virion-free HIV-CM was 26.60 pg/ml (1.9 pM) as measured using ELISA, rVpr was used at two concentrations: 2.0 pM (approximately equal to the highest concentration of Vpr in HIV-CM, designated Vpr-2.0) and 10 pM (Vpr-10). The progenitor cells were cultured in CM containing rVpr and were analyzed for neurite outgrowth. Neurite outgrowth was clearly inhibited in a dose-dependent manner (Fig. 2A and B). As shown in Fig. 2B, at 72 h in culture, the mean length of primary neurites was 176.70 ± 13.75 μm (C-CM), 105.97 ± 6.28 μm (Vpr-2.0), and 85.83 ± 17.46 μm (Vpr-10) (Fig. 2B). When anti-Vpr antibody was added to the culture prior to the addition of rVpr, Vpr-induced inhibition of neurite outgrowth was clearly blocked (percentage of suppression, 68.50%; no statistical significance was found compared to results for the control group) (Fig. 2C).

To examine whether Vpr inhibits axon and neuronal polarity formation, progenitor cells were plated and cultured in the presence of C-CM, Vpr-2.0, or Vpr-10. We randomly selected 100 cells in each culture and classified them into the three developmental stages. At 24 h, more than half of them were in stage 2, independent of the CM (Fig. 2D). At 48 h, the percentage of stage 3 progenitor cells was 64.9% ± 2.62% in cells cultured with C-CM, while the percentage was significantly lower in the presence of rVpr (Vpr-2.0, 29.67% ± 4.04%; Vpr-10, 28.00% ± 3.00%). A considerably large fraction of cells remained in stage 2 (Vpr-2.0, 64.33% ± 1.53%; Vpr-10, 63.33% ± 3.21%) when exposed to rVpr (Fig. 2E). These results confirm that the soluble form of Vpr protein induces

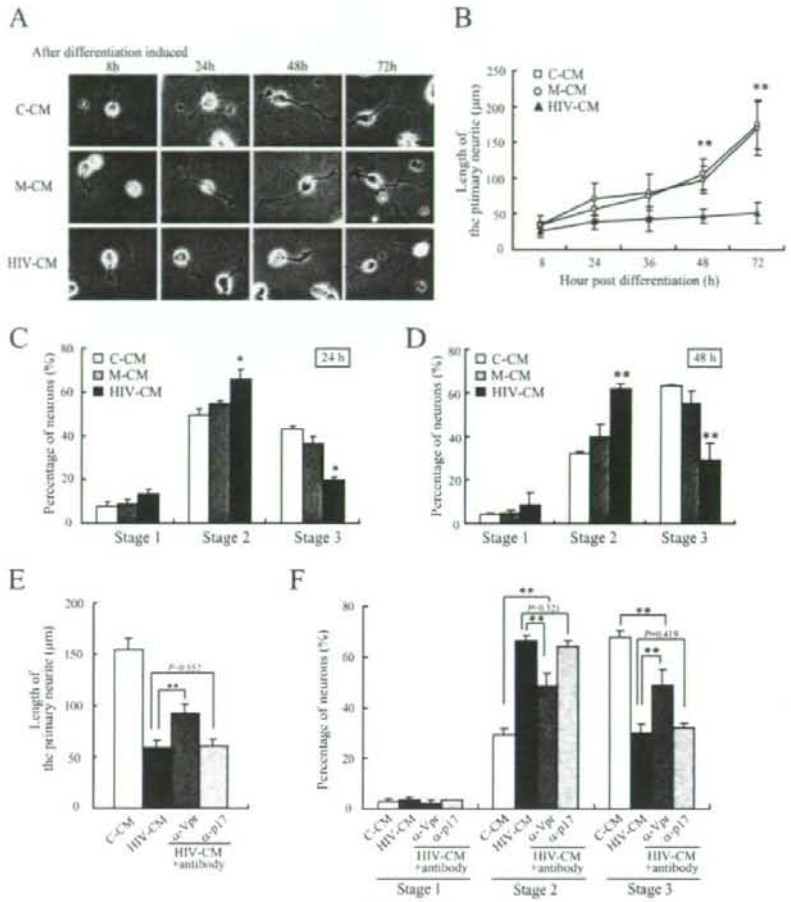

FIG. 1. Impairment of axonal growth by HIV-1-infected MDM. (A) The neurite outgrowth of neurons cultured in C-CM, M-CM, or HIV-CM was monitored for 72 h in differentiation cultures of neuronal progenitor cells. Phase-contrast images were obtained using a 40× objective. Scale bars, 20 μm. (B) The length of the primary neurite of each cell was measured in the culture. **, $P < 0.01$ compared to results for C-CM and M-CM cultures. (C and D) Progenitor cells under each condition were classified into three developmental stages as described in Materials and Methods at 24 h (C) and 48 h (D) in culture. *, $P < 0.05$ compared to results for C-CM and M-CM cultures. (E) Progenitor cells were cultured with C-CM, HIV-CM, or HIV-CM supplemented with anti-Vpr antibody (260 ng/ml; HIV-CM+anti-Vpr) or anti-$p17^{MA}$ antibody (260 ng/ml; HIV-CM+anti-p17), and the length of the primary neurite was measured. **, $P < 0.01$. (F) The cells under each condition were classified into three developmental stages. **, $P < 0.01$.

the inhibition of axon formation in a manner similar to that of HIV-CM.

Mitochondrial membrane depolarization of neurons caused by Vpr. Mitochondria play important roles in neuronal developmental processes, including the establishment of axon polarity and the regulation of neurite outgrowth (36, 37). Since it has been reported that Vpr influences mitochondrial function in several cell types and induces mitochondrial membrane depolarization (5, 25, 26), Vpr also may induce mitochondrial dysfunction in neuronal progenitor cells. To elucidate the mechanism of Vpr-induced mitochondrial dysfunction, we added serially increasing concentrations of rVpr, from 0.2 pM to 1.0 nM, to progenitor cell cultures and measured the $\Delta\Psi m$ in live neuronal progenitor cells using staining with JC-1. As shown in Fig. 3A, the $\Delta\Psi m$ clearly decreased in rVpr-treated cells in a dose-dependent manner, indicating that Vpr also affected the $\Delta\Psi m$ in neuronal progenitor cells.

Mitochondrial membrane depolarization has been shown to reduce ATP production (10). The proper transport of mitochondria within axons or neurites needs its motor proteins, and the motor proteins utilize ATP for its mobilization (10, 21). As shown in Fig. 3B, the concentration of cellular ATP was significantly reduced by exposure to 2.0 pM rVpr (1.50 ± 0.56 μM) compared to that in C-CM-cultured progenitor cells (4.57 ± 0.79 μM).

Although mitochondrial membrane depolarization and the